

Cosmological implications of anisotropic clustering measurements in BOSS and eBOSS



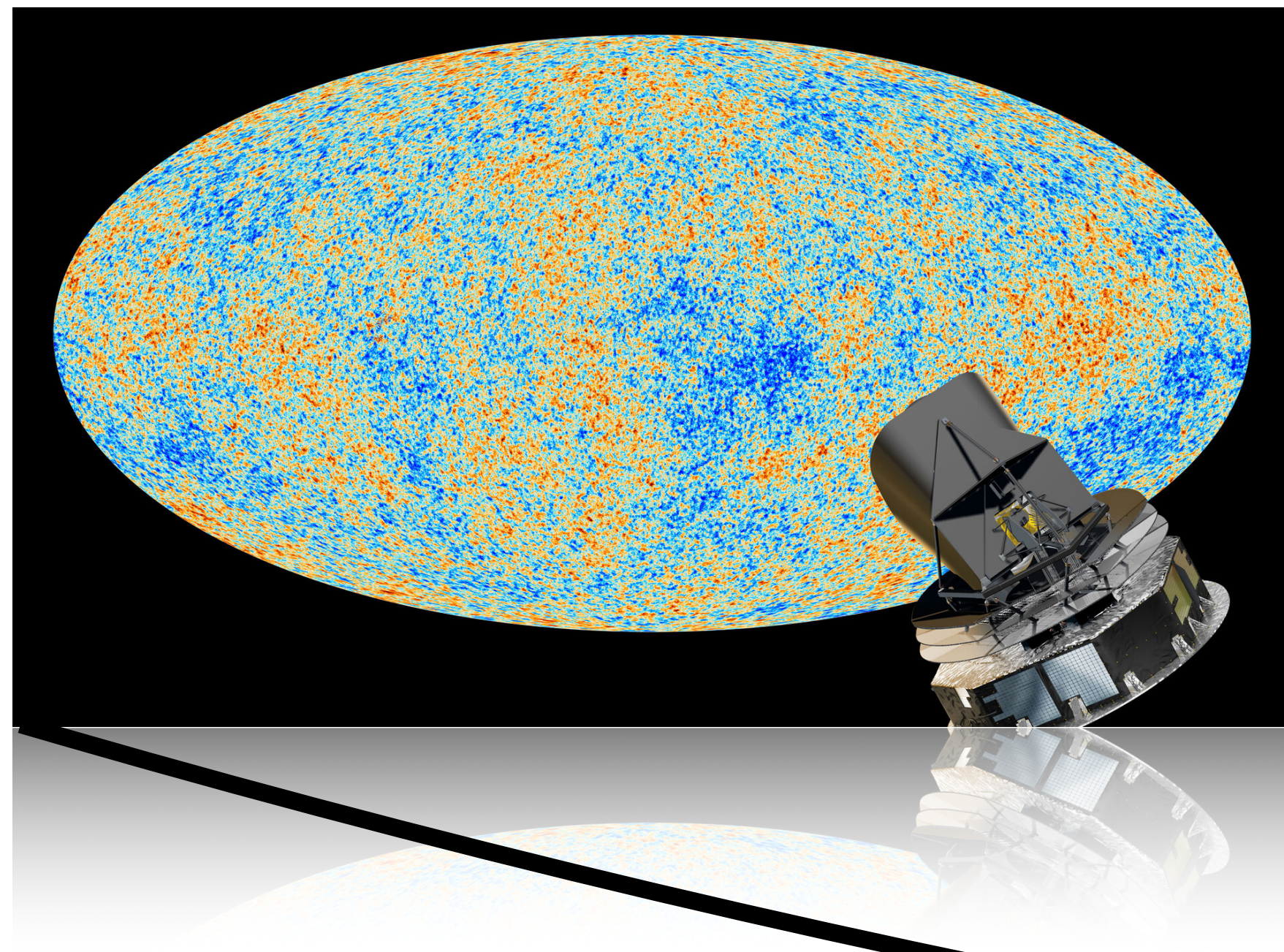
Agnė Semėnaitė

Ariel G. Sánchez, Andrea Pezzotta and eBOSS collaboration

arXiv: 2111.03156

Planck - the cosmological standard

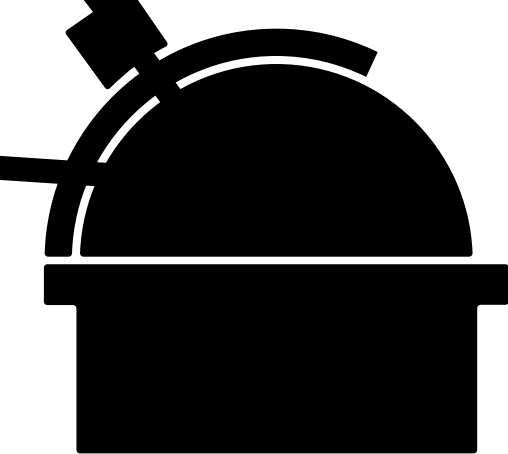
$z = 1100$



The cosmic microwave background signature gives the most precise measurements of cosmological parameters to date.

Λ CDM:

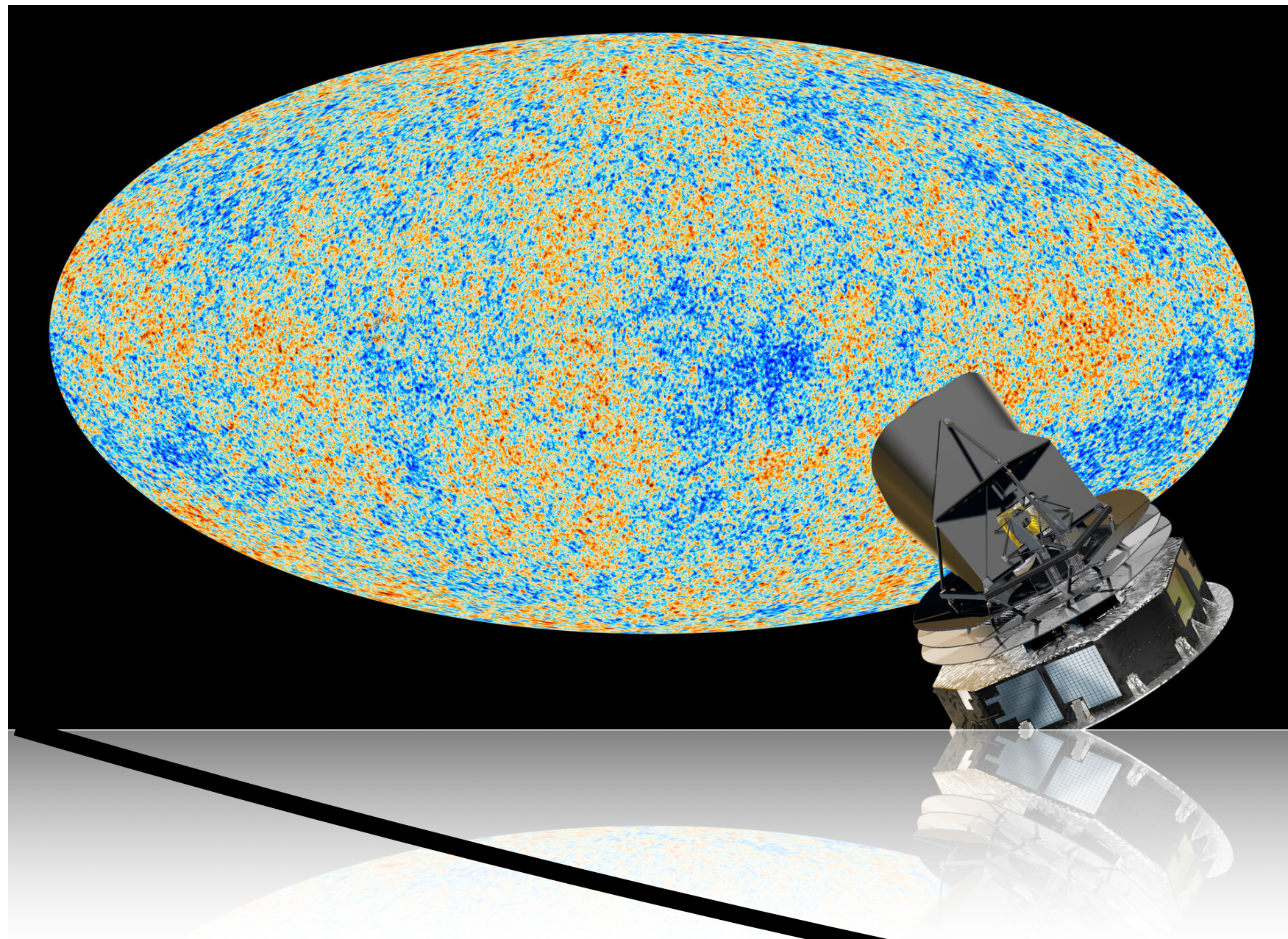
$\Omega_c h^2, \Omega_b h^2, H_0, n_s, A_s, \tau$



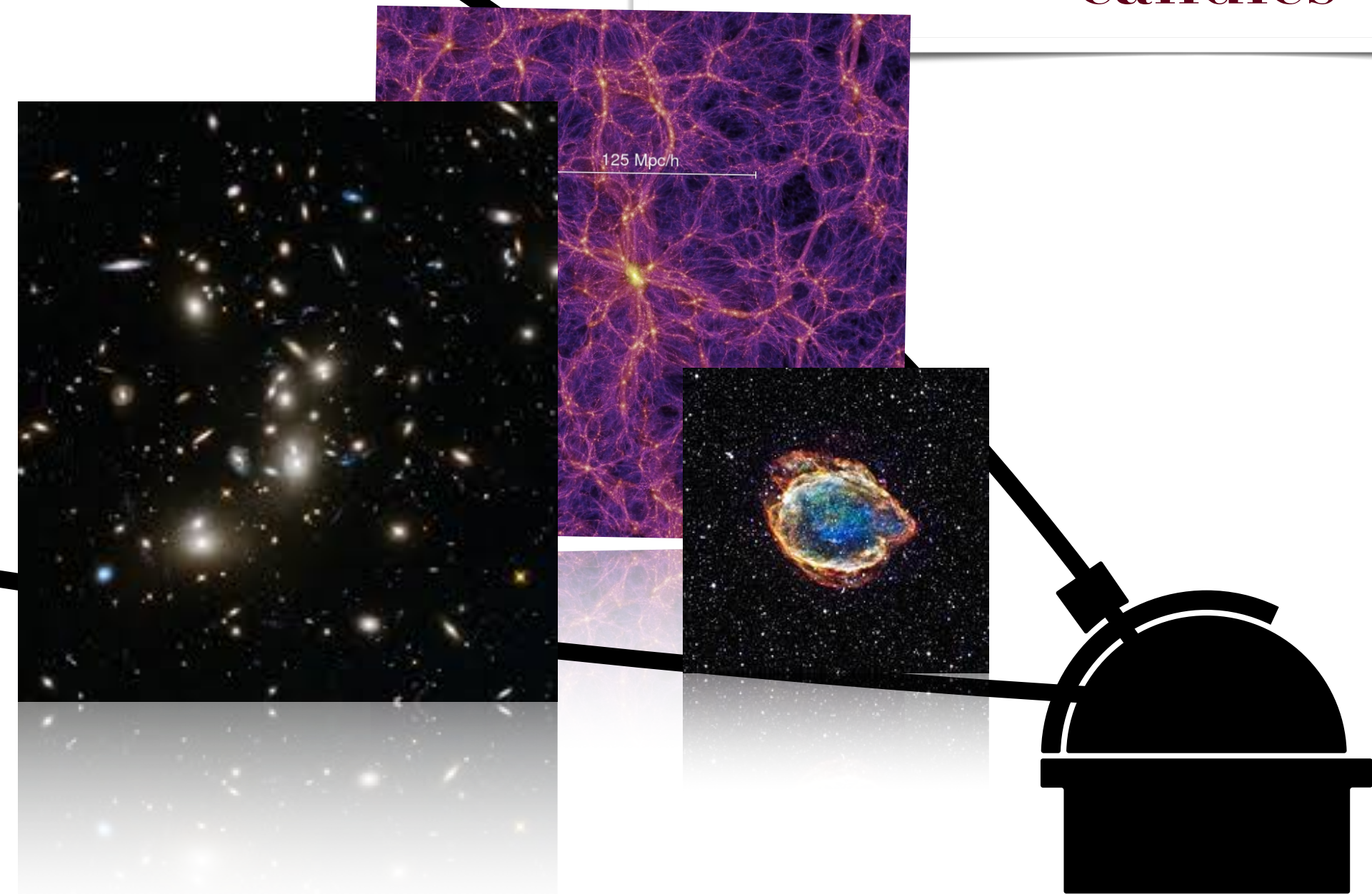
$z = 0$

Planck - the cosmological standard

$z = 1100$



We can compare Planck's predictions for the low redshift universe with our observations of the large scale structure or direct measurements using standard candles

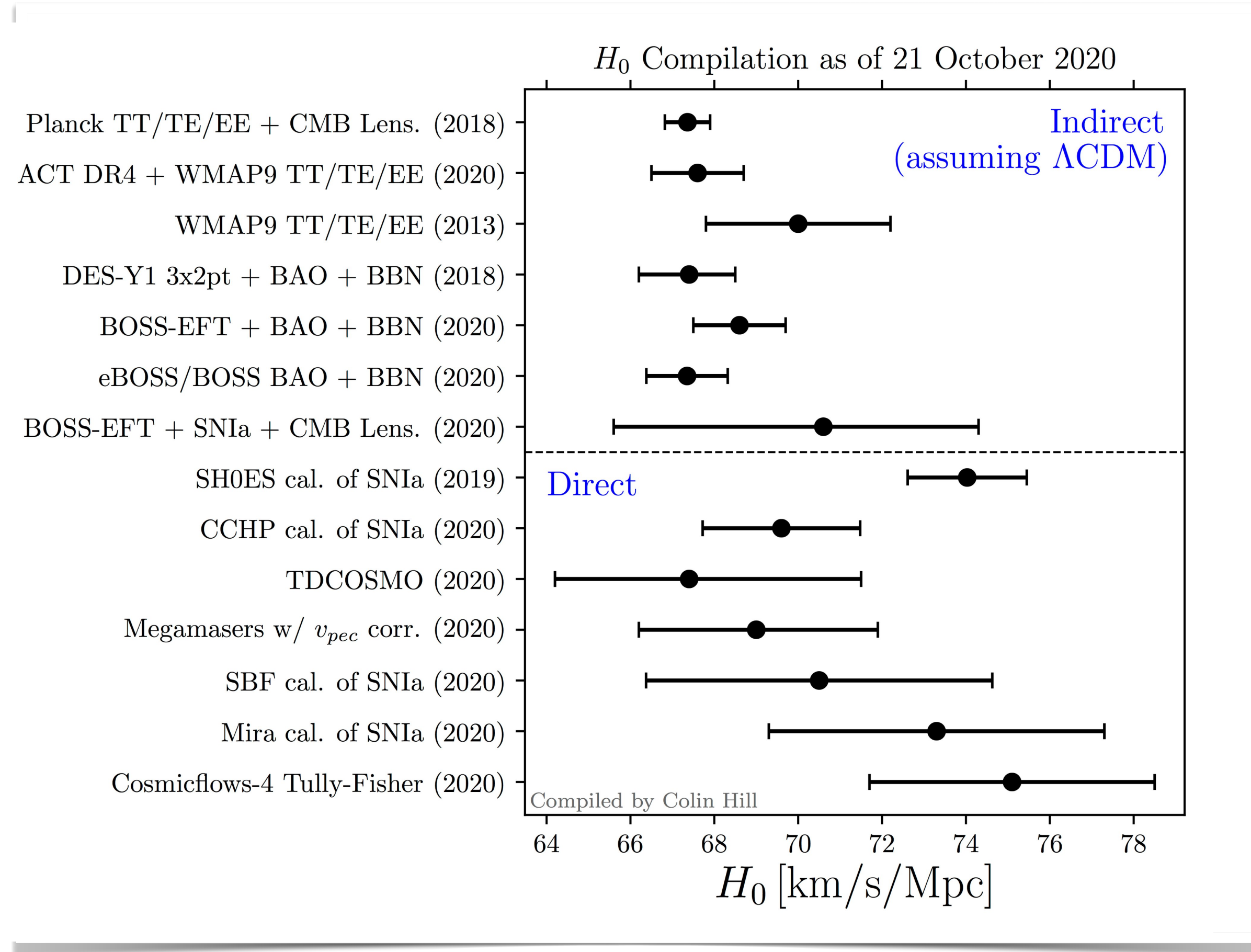
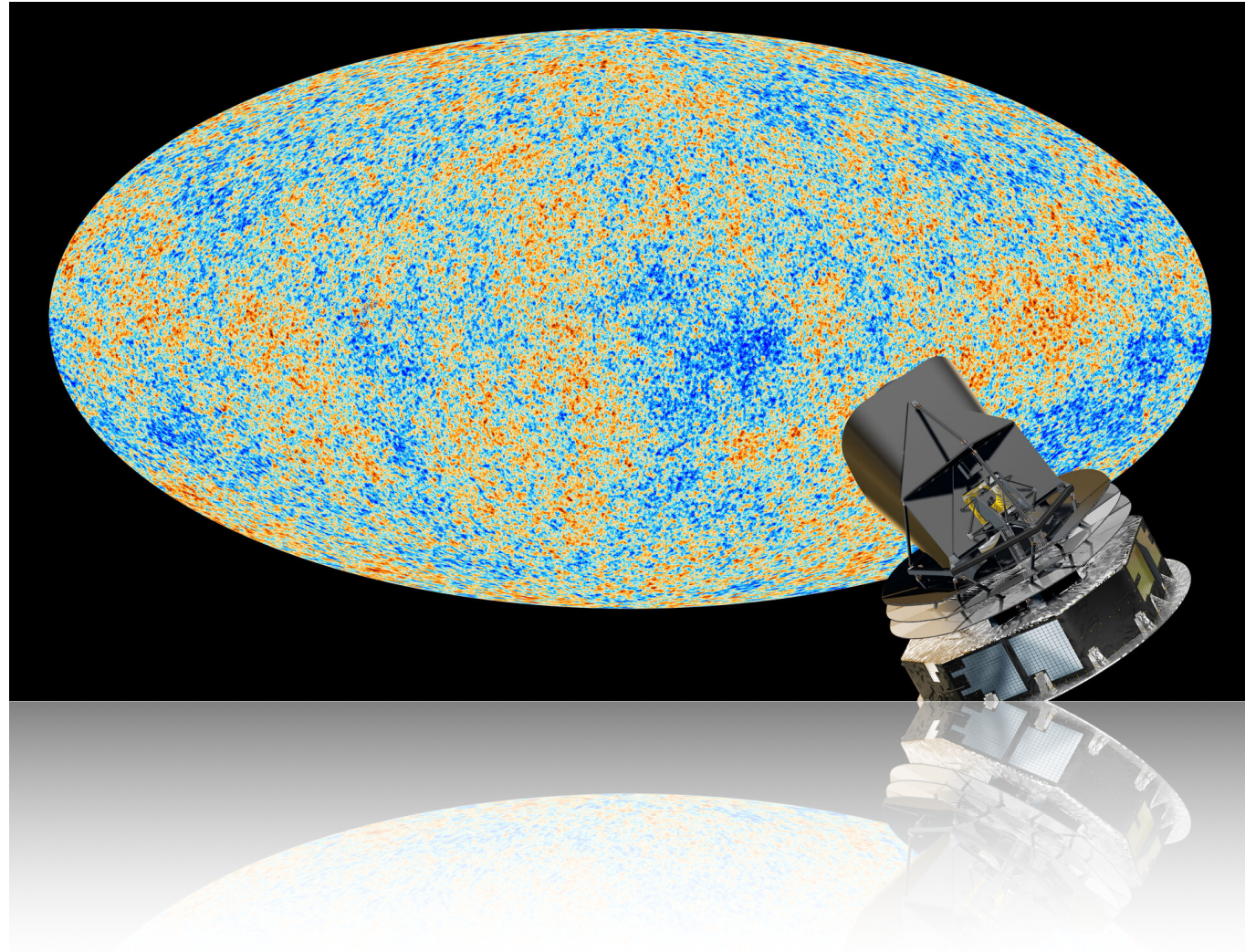


$z = 0$

Λ CDM:

$\Omega_c h^2, \Omega_b h^2, H_0, n_s, A_s, \tau$

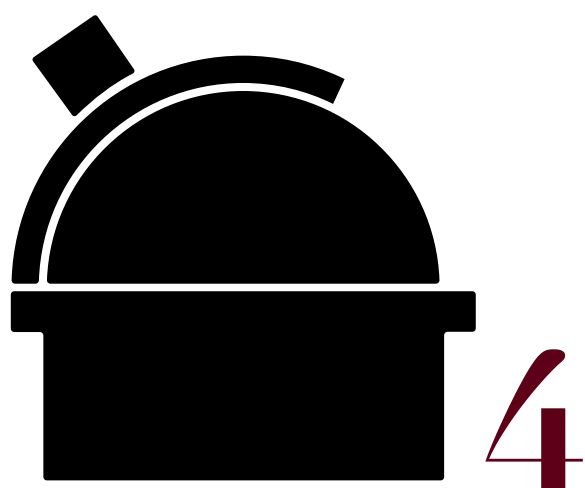
Cracks in the model?



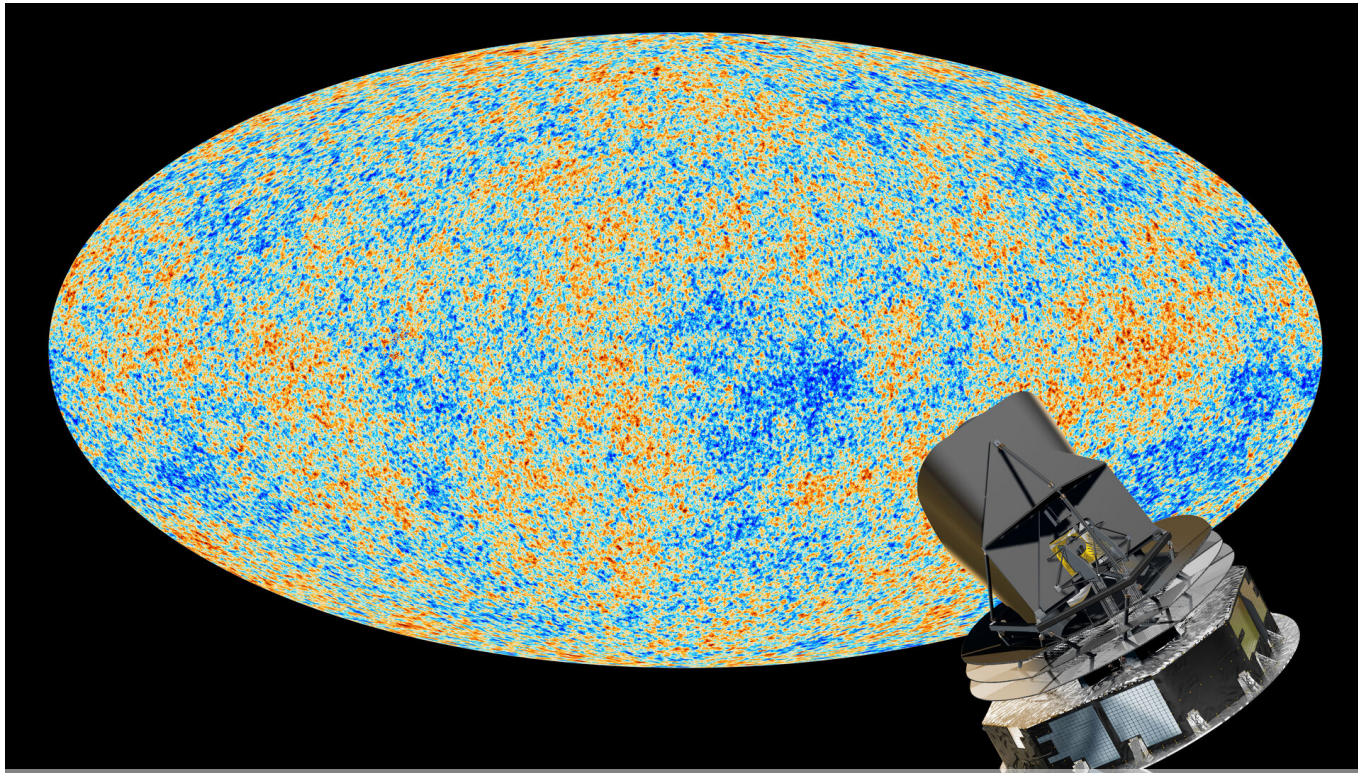
?

Image: Colin Hill

- ▶ The rate of expansion of the Universe today, as measured directly seems to be greater than Planck's prediction...



Cracks in the model?



► Planck also predicts a higher lensing amplitude than measured by weak lensing surveys.

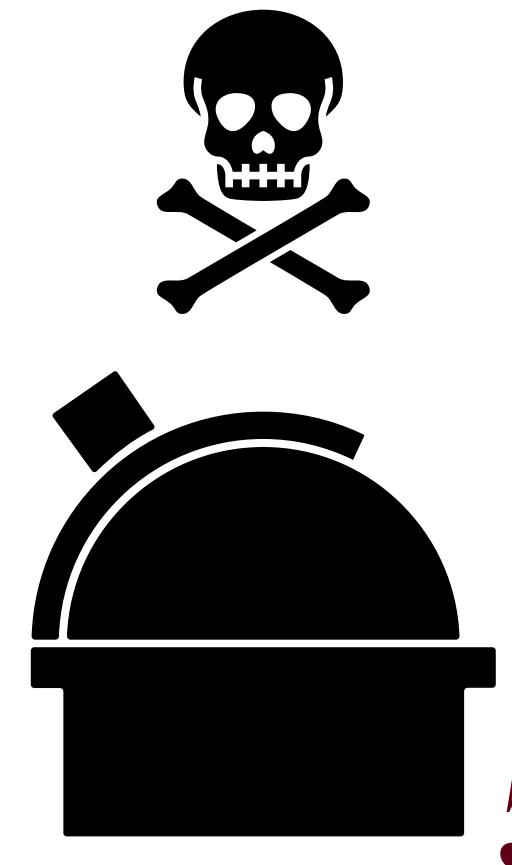
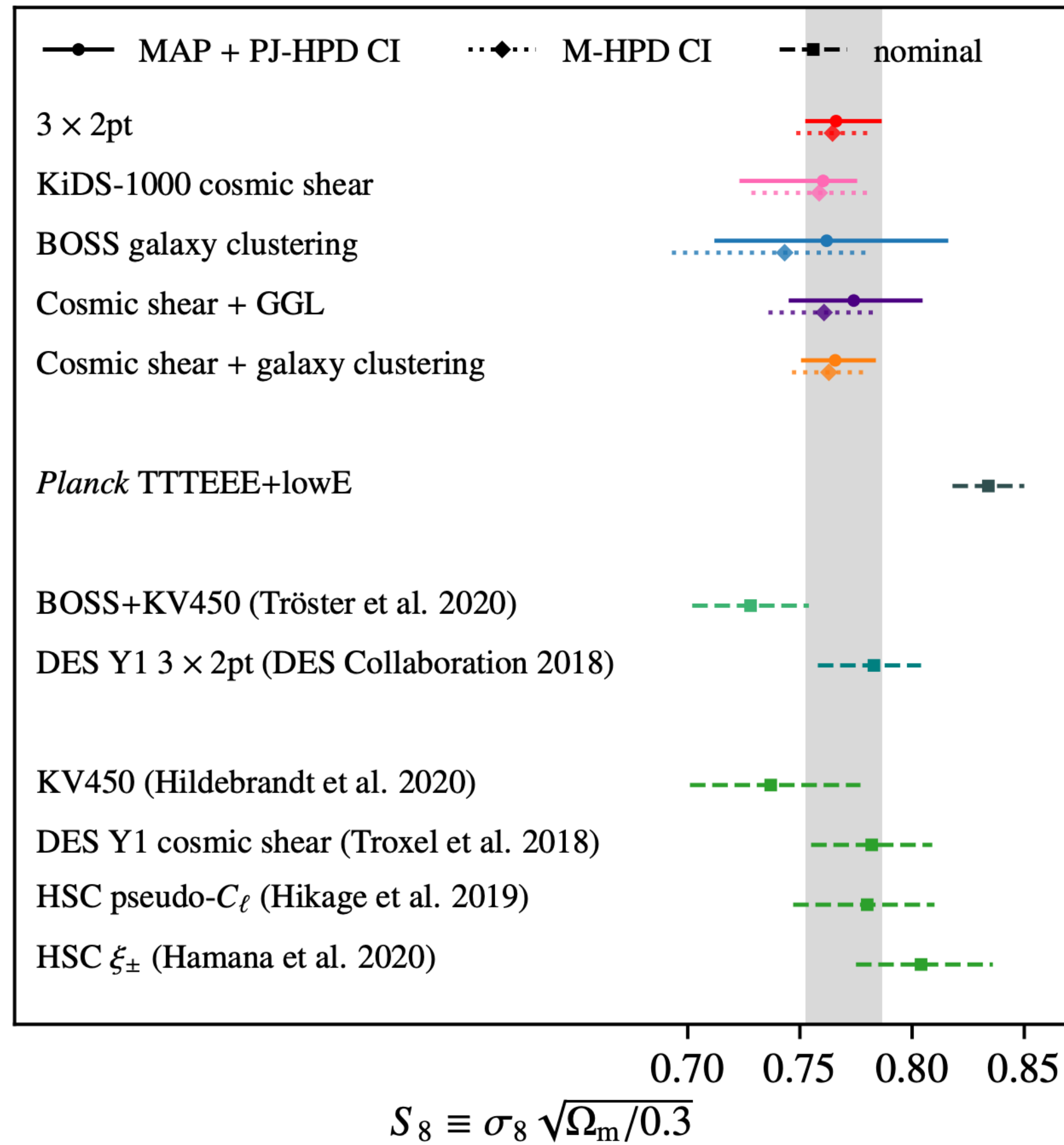
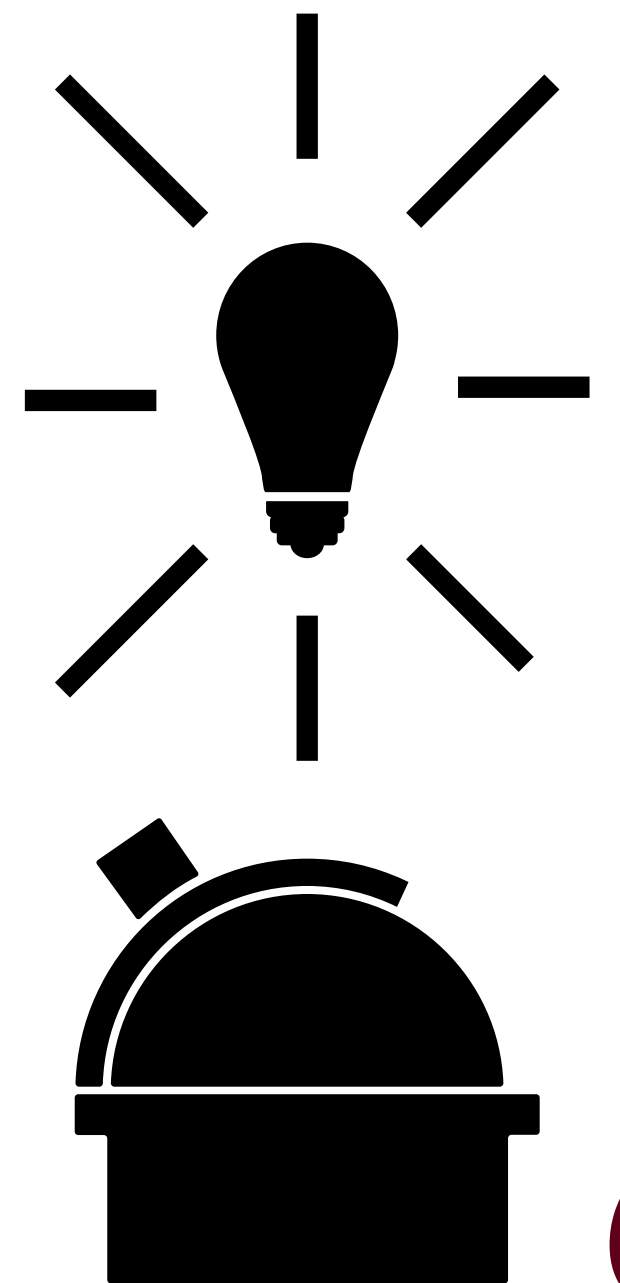
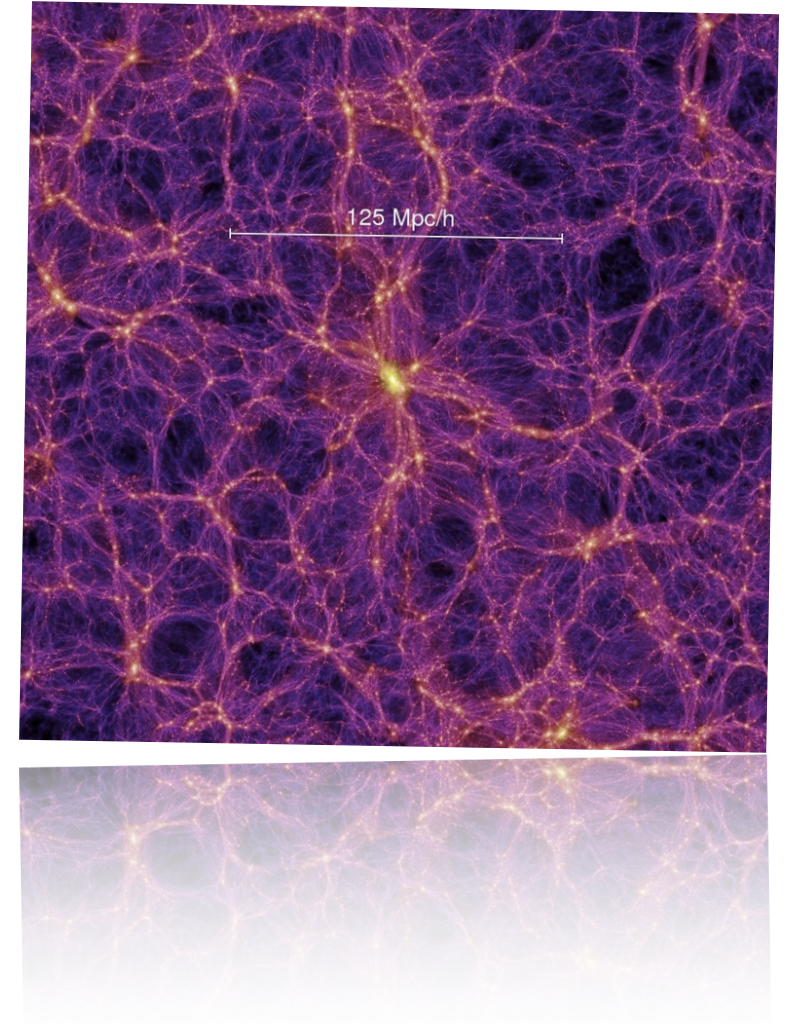


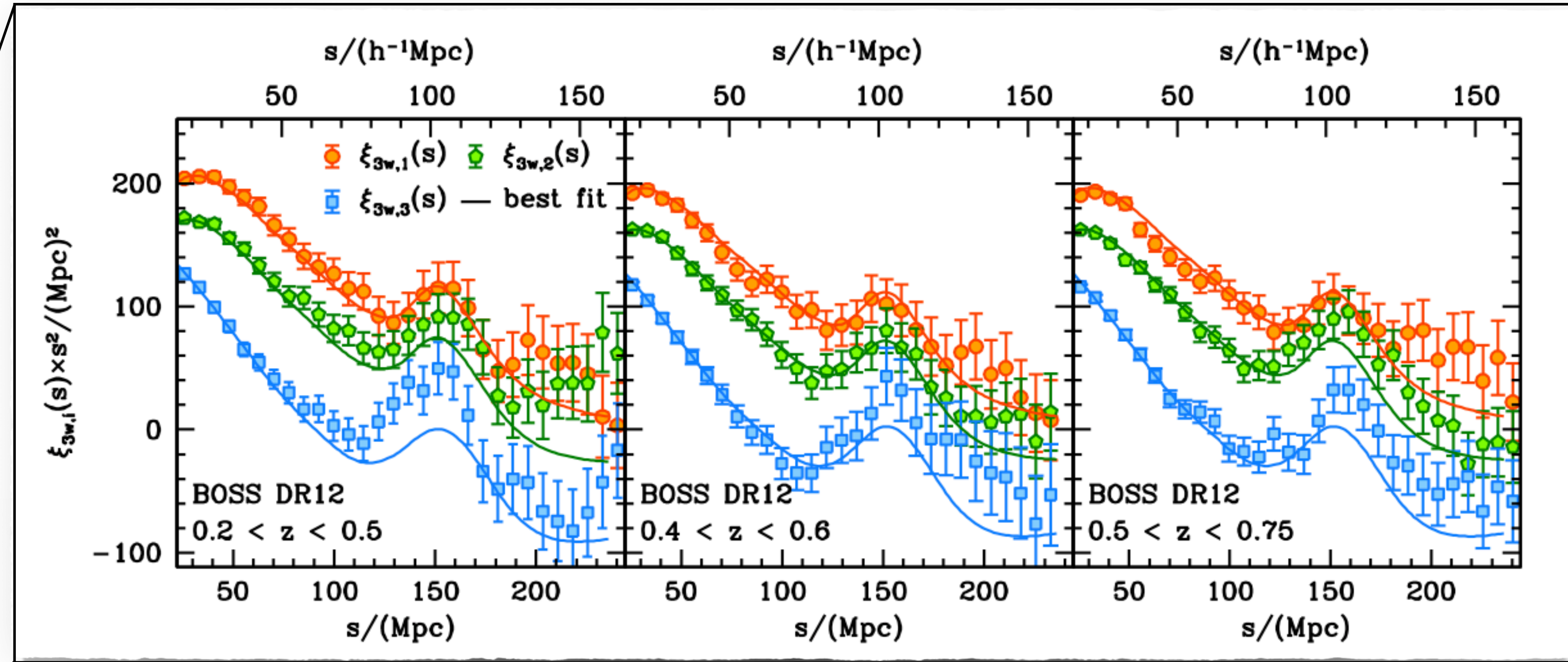
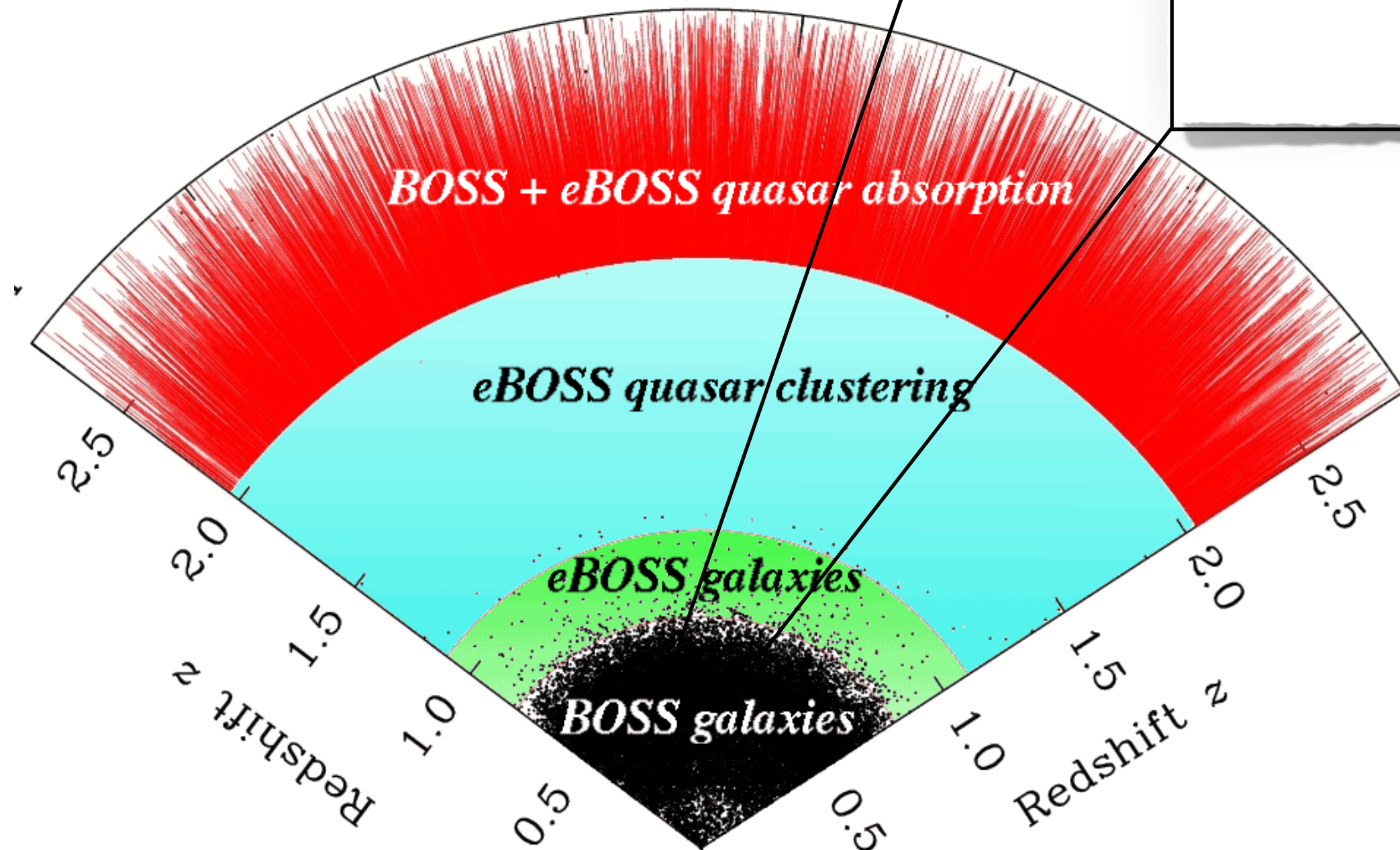
Image: Heymans, Tröster & the KiDS Collaboration

This work:

- ⦿ We present full shape eBOSS quasar clustering analysis.
- ⦿ Combine with full shape BOSS galaxy clustering wedges re-analysis with an updated model for power spectrum and bias modelling.
- ⦿ Obtain combined large scale structure constraints for the low redshift Universe by complimenting the clustering measurements with weak lensing and clustering measurements (3x2pt) from Dark Energy Survey, Year 1 data release.



Clustering measurements *Sánchez et al., 2017*



- **BOSS clustering wedges**, 2 redshift bins to avoid overlapping: low- z and high- z . $\xi_{\mu_1}^{\mu_2} = \frac{1}{\Delta\mu} \int_{\mu_1}^{\mu_2} \xi(\mu, s) d\mu$

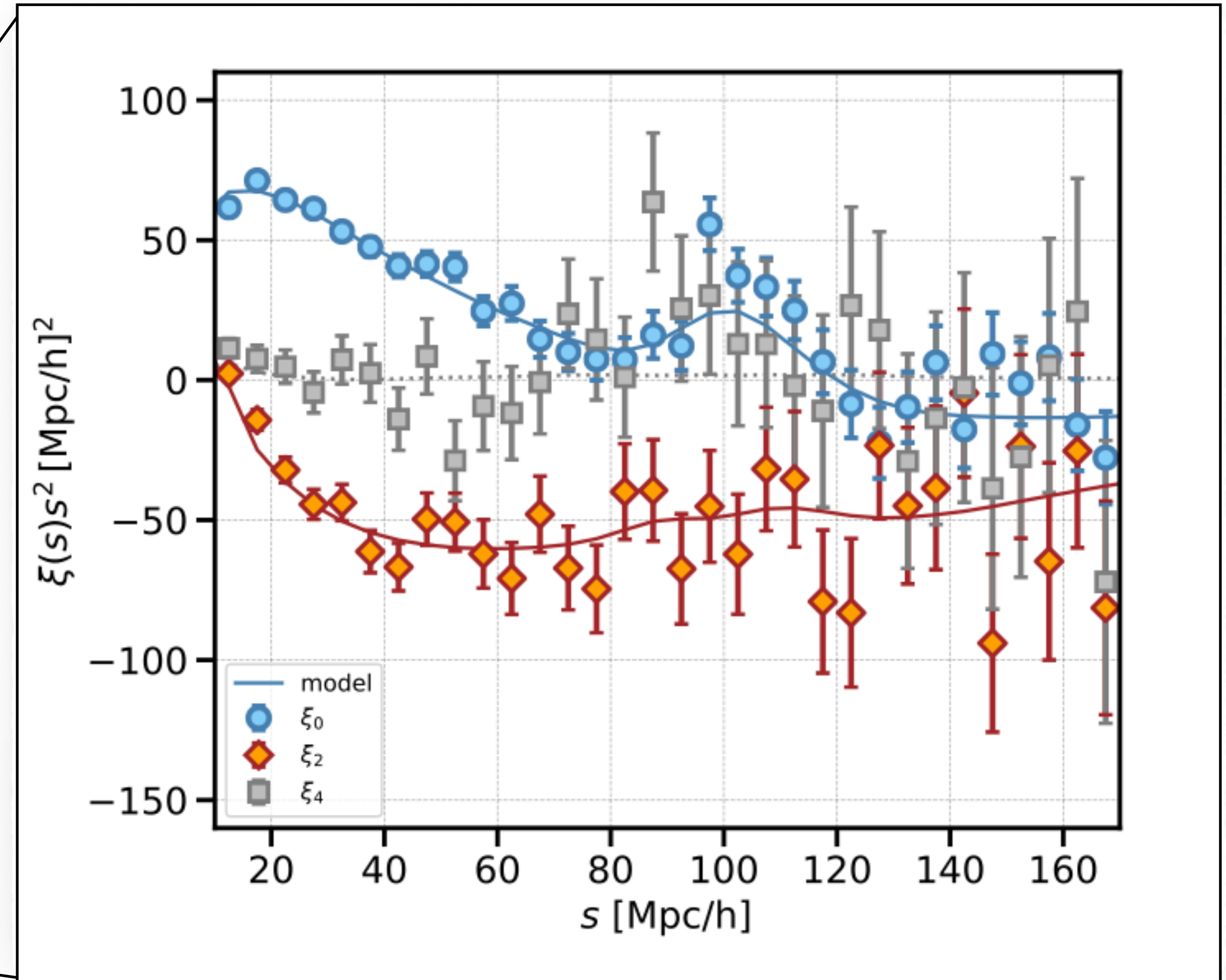
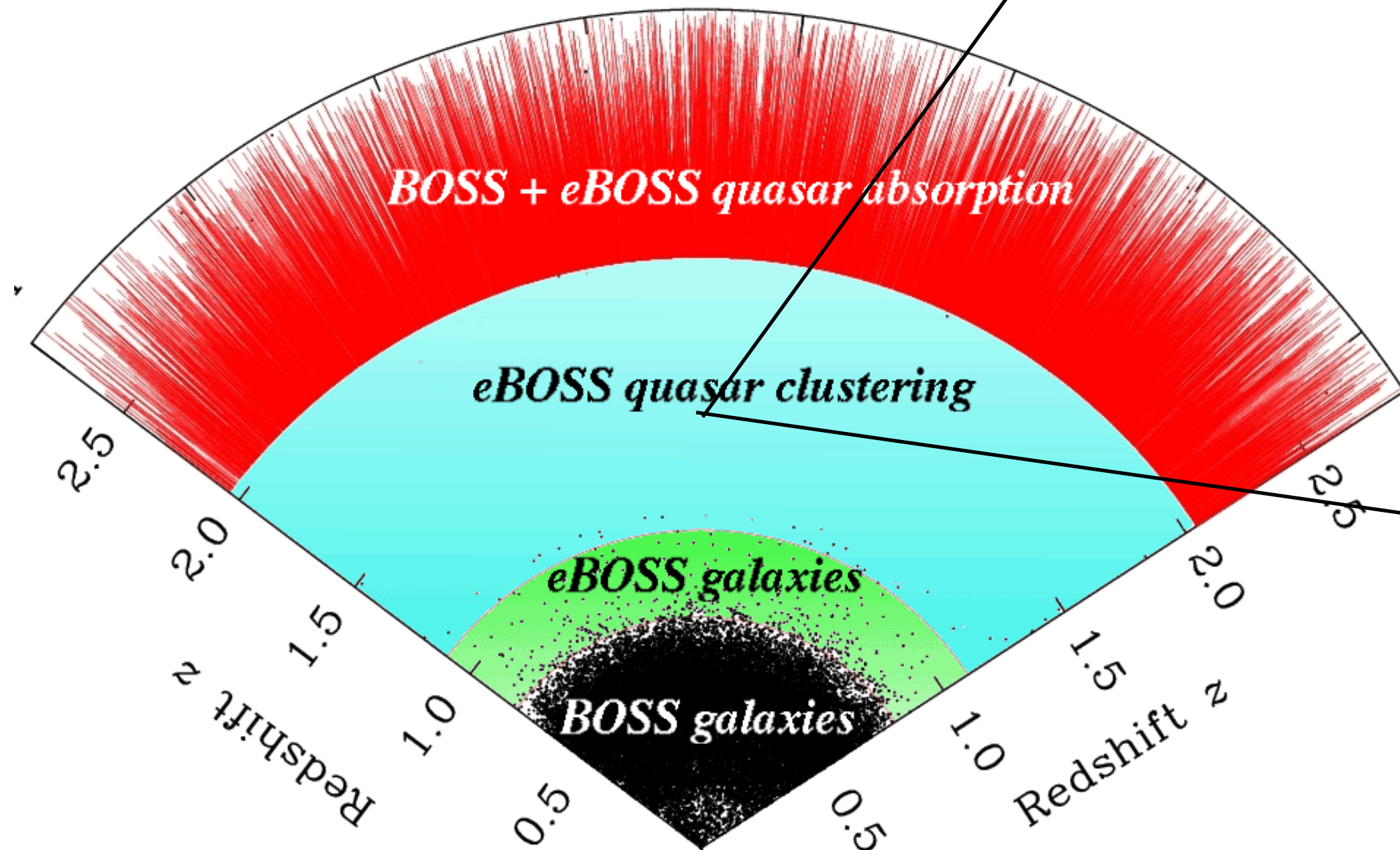
Clustering measurements

Hou et al., 2020

- **eBOSS** quasar clustering
multipoles one redshift bin:

$$0.8 < z < 2.2$$

$$\xi_l(s) = \frac{2l+1}{2} \int_{-1}^1 L_l(\mu) \xi(\mu, s) d\mu$$



Modelling

Non-linear clustering:

$$P(k, \mu)$$

Galaxy bias:

RSD:

Modelling

Non-linear clustering:

Galaxy bias:

$$P(k, \mu) = W_{\infty}(ifk\mu) P_{\text{novir}}(k, \mu)$$

RSD:

● Taruya, Nishimichi, Saito (2010) + Scoccimarro (2004).

$$W_{\infty}(\lambda) = \frac{1}{\sqrt{1 - \lambda^2 a_{\text{vir}}^2}} \exp\left(\frac{\lambda^2 \sigma_v^2}{1 - \lambda^2 a_{\text{vir}}^2}\right)$$

Modelling

Non-linear clustering:

- **RESPRESSO** - matter power spectrum predictions based on response function approach (Nishimichi et al. 2017)

Galaxy bias:

$$P(k, \mu) = W_\infty(ik\mu) P_{\text{novir}}(k, \mu)$$

RSD:

- Taruya, Nishimichi, Saito (2010) + Scoccimarro (2004).

$$W_\infty(\lambda) = \frac{1}{\sqrt{1 - \lambda^2 a_{\text{vir}}^2}} \exp\left(\frac{\lambda^2 \sigma_v^2}{1 - \lambda^2 a_{\text{vir}}^2}\right)$$

Modelling

Non-linear clustering:

- **RESPRESSO** - matter power spectrum predictions based on response function approach (Nishimichi et al. 2017)

Galaxy bias:

- One loop bias + **co-evolution** relations (Eggemeier et al., 2019)

$$\delta = b_1 \delta_m + \frac{b_2}{2!} \delta_m^2 + \gamma_2 \mathcal{G}_2(\Phi_v) + \gamma_{21} \mathcal{G}_2(\varphi_1, \varphi_2) + \dots$$

$$\gamma_{2,\text{ex}} = 0.524 - 0.547b_1 + 0.046b_1^2$$

$$\gamma_{21} = -\frac{2}{21}(b_1 - 1) + \frac{6}{7}\gamma_2.$$

$$P(k, \mu) = W_\infty(ik\mu) P_{\text{novir}}(k, \mu)$$

RSD:

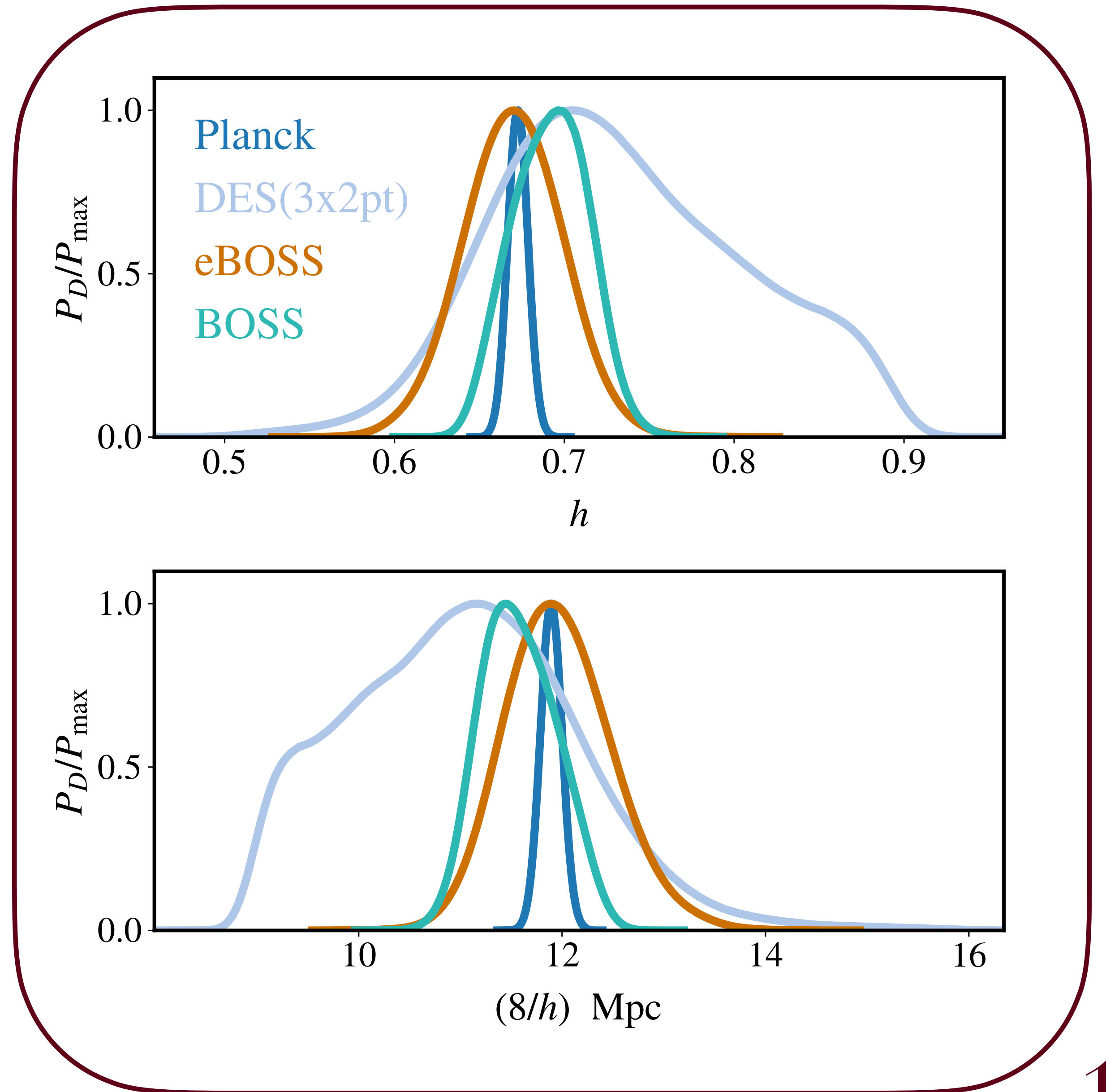
- Taruya, Nishimichi, Saito (2010) + Scoccimarro (2004).

$$W_\infty(\lambda) = \frac{1}{\sqrt{1 - \lambda^2 a_{\text{vir}}^2}} \exp\left(\frac{\lambda^2 \sigma_v^2}{1 - \lambda^2 a_{\text{vir}}^2}\right)$$

Parameter space

Sánchez (2020)

- Different probes recover different posteriors for Hubble parameter $h = H_0/100$.



Parameter space

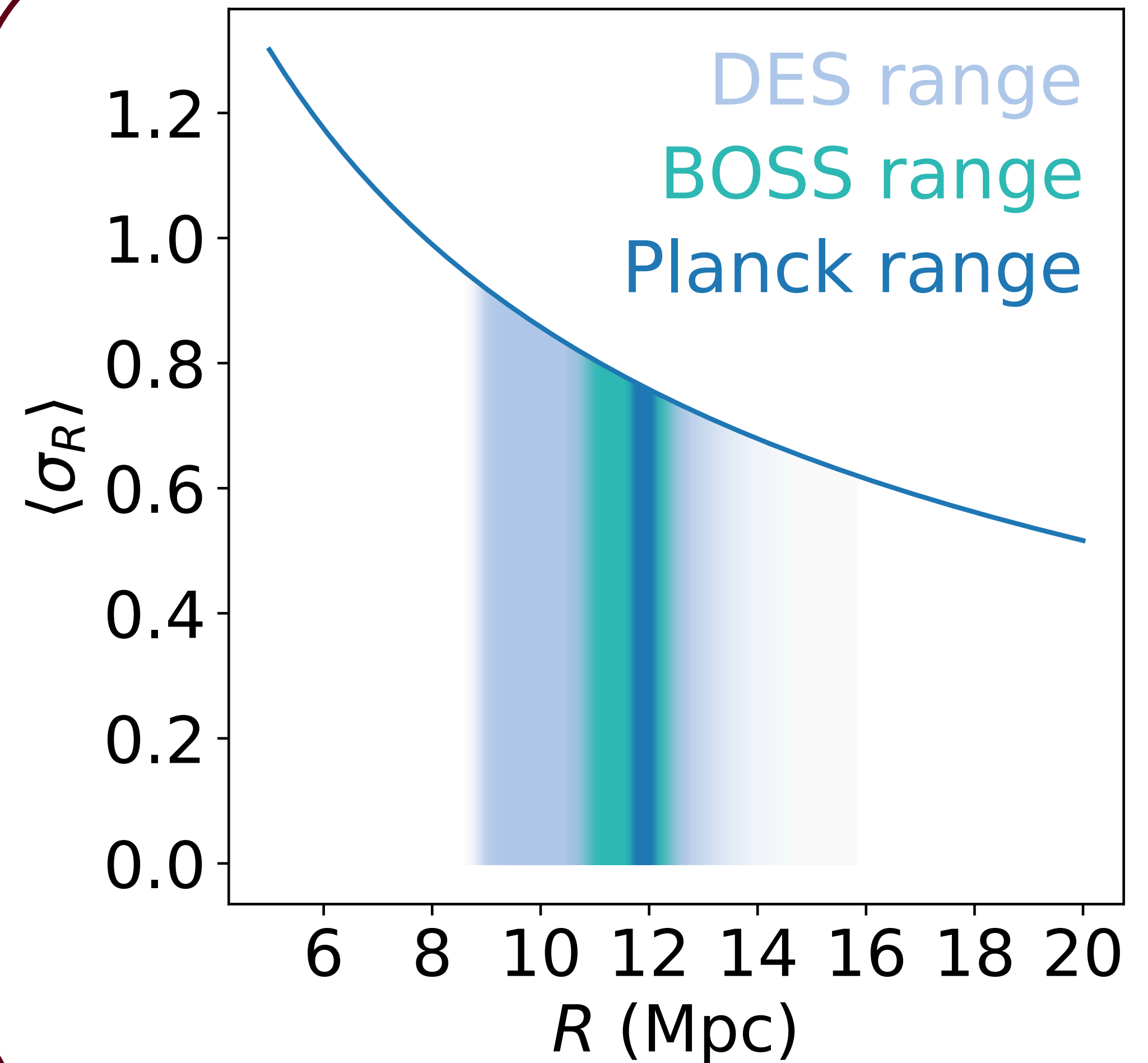
Sánchez (2020)

- When we define a parameter through h units, the measured value gives a weighted average of the quantity over h ($h = H_0/100$).

σ_8 measured in radius of $8 h^{-1}\text{Mpc}$

$$\Omega_m = \omega_m / h^2$$

$$\Omega_{DE} = \omega_{DE} / h^2$$



Parameter space

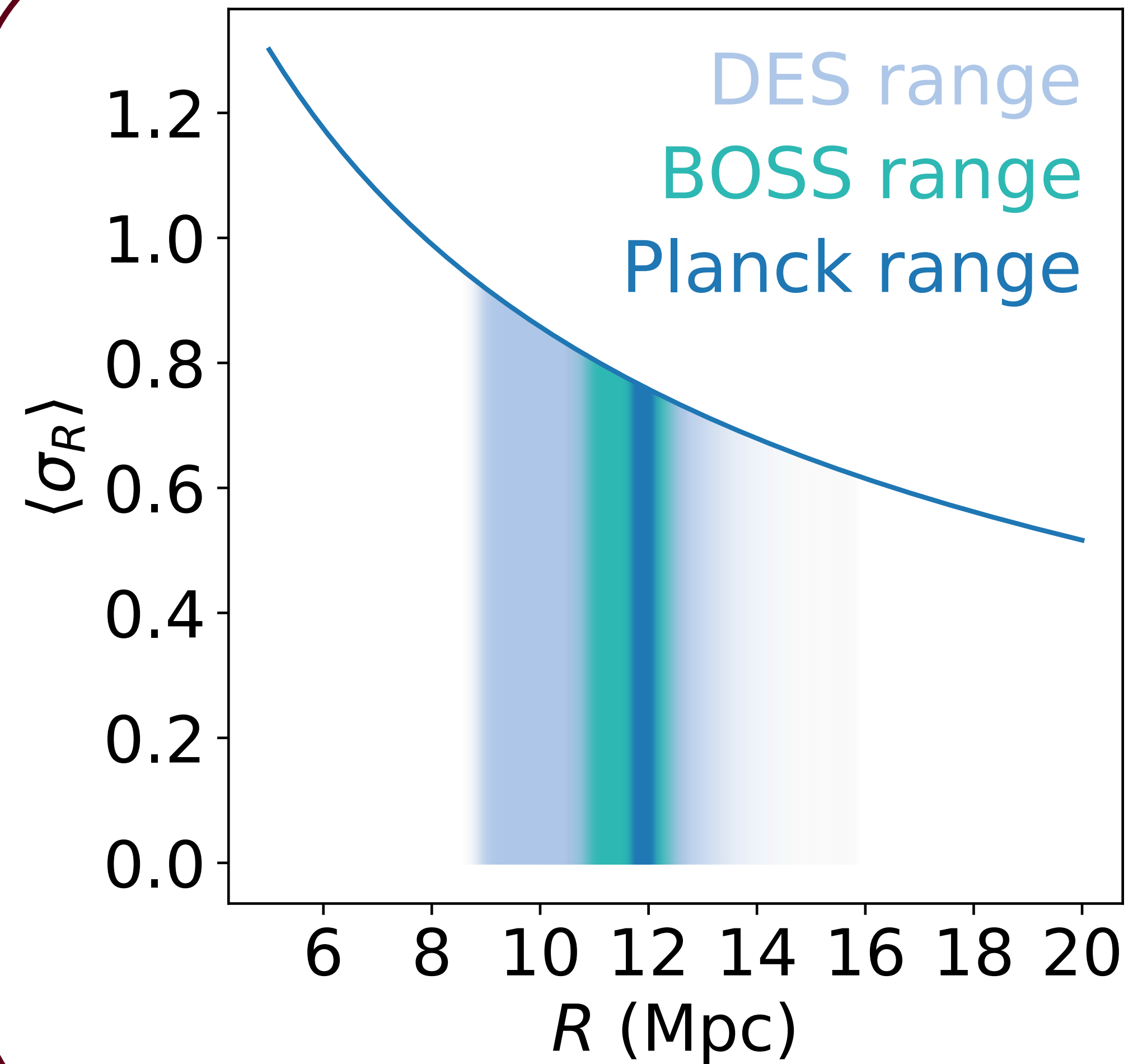
Sánchez (2020)

- When we define a parameter through h units, the measured value gives a weighted average of the quantity over h ($h = H_0/100$).

σ_{12} measured in radius of 12 Mpc

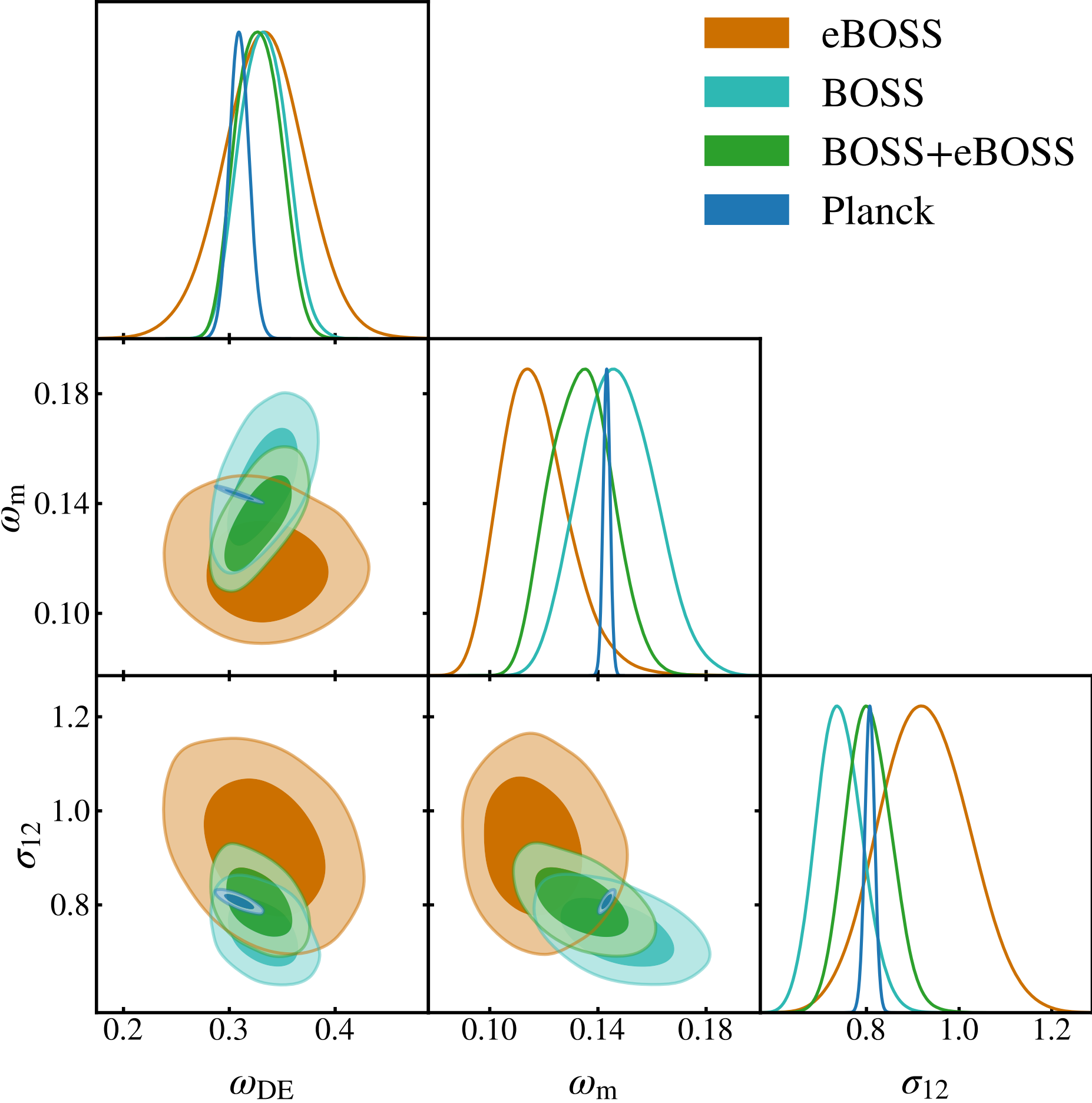
$$\omega_m = 8\pi G\rho_m / (3H_{100}^2) \quad 100 \text{ km s}^{-1} \text{ Mpc}^{-1}$$

$$\omega_{\text{DE}} = 8\pi G\rho_{\text{DE}} / (3H_{100}^2)$$



Results: BOSS+eBOSS

Results: BOSS+eBOSS



Joint constraints are in an excellent agreement with Planck:

⊙ Suspiciousness: $0.64 \pm 0.07\sigma$

$$\sigma_{12} = 0.805 \pm 0.049$$
$$(\sigma_8 = 0.814 \pm 0.044)$$

Results: BOSS+eBOSS

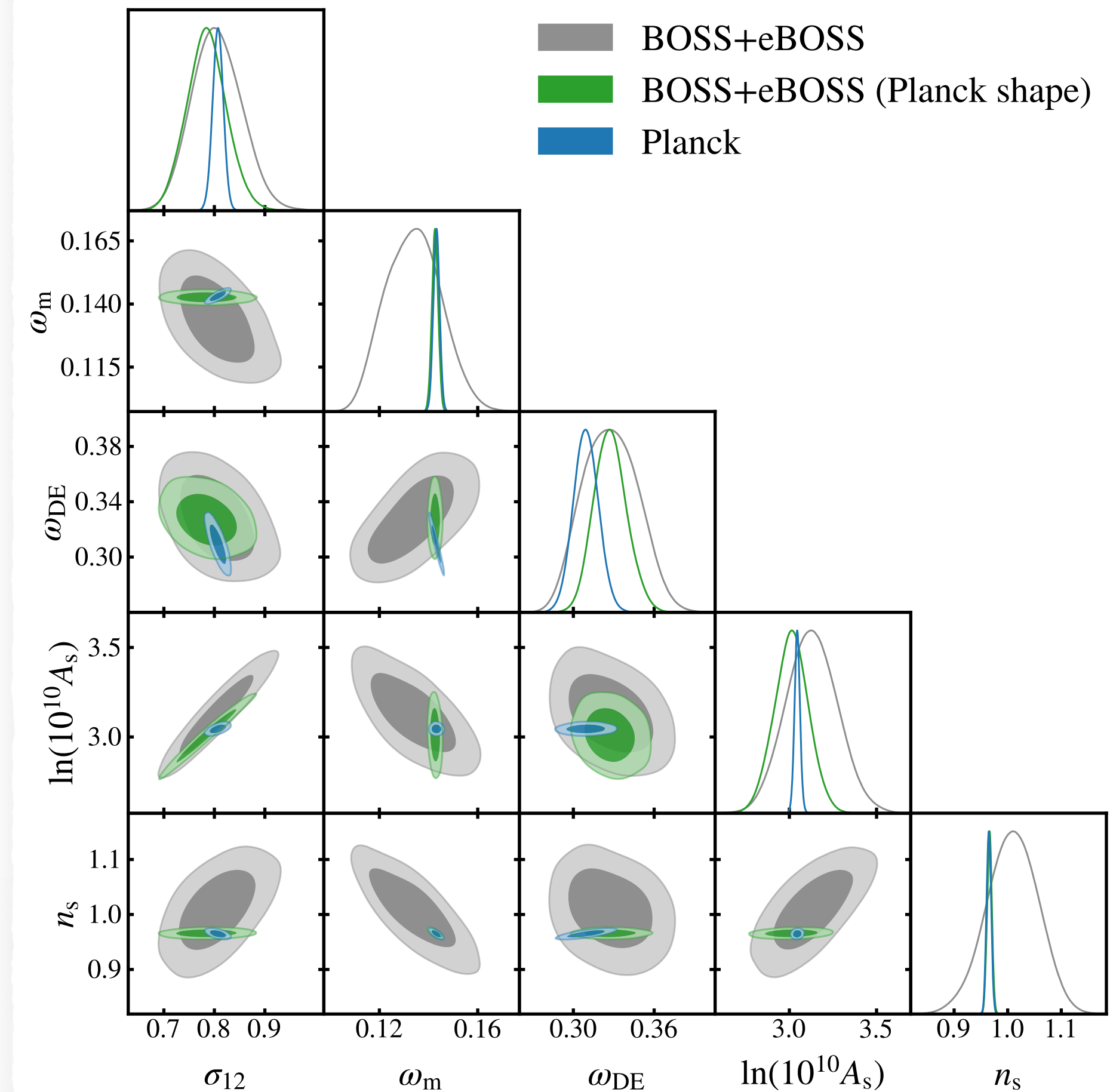
Sánchez et al. (2021) distinguishes between *shape* and *evolution* parameters.

- ⦿ We want to test the effect of a prior on **shape** parameters ω_b , ω_{cdm} and n_s .
- ⦿ We explore the impact it has on **evolution** parameters σ_{12} , A_s , ω_{DE} .

Results: BOSS+eBOSS

Sánchez et al. (2021) distinguishes between *shape* and *evolution* parameters.

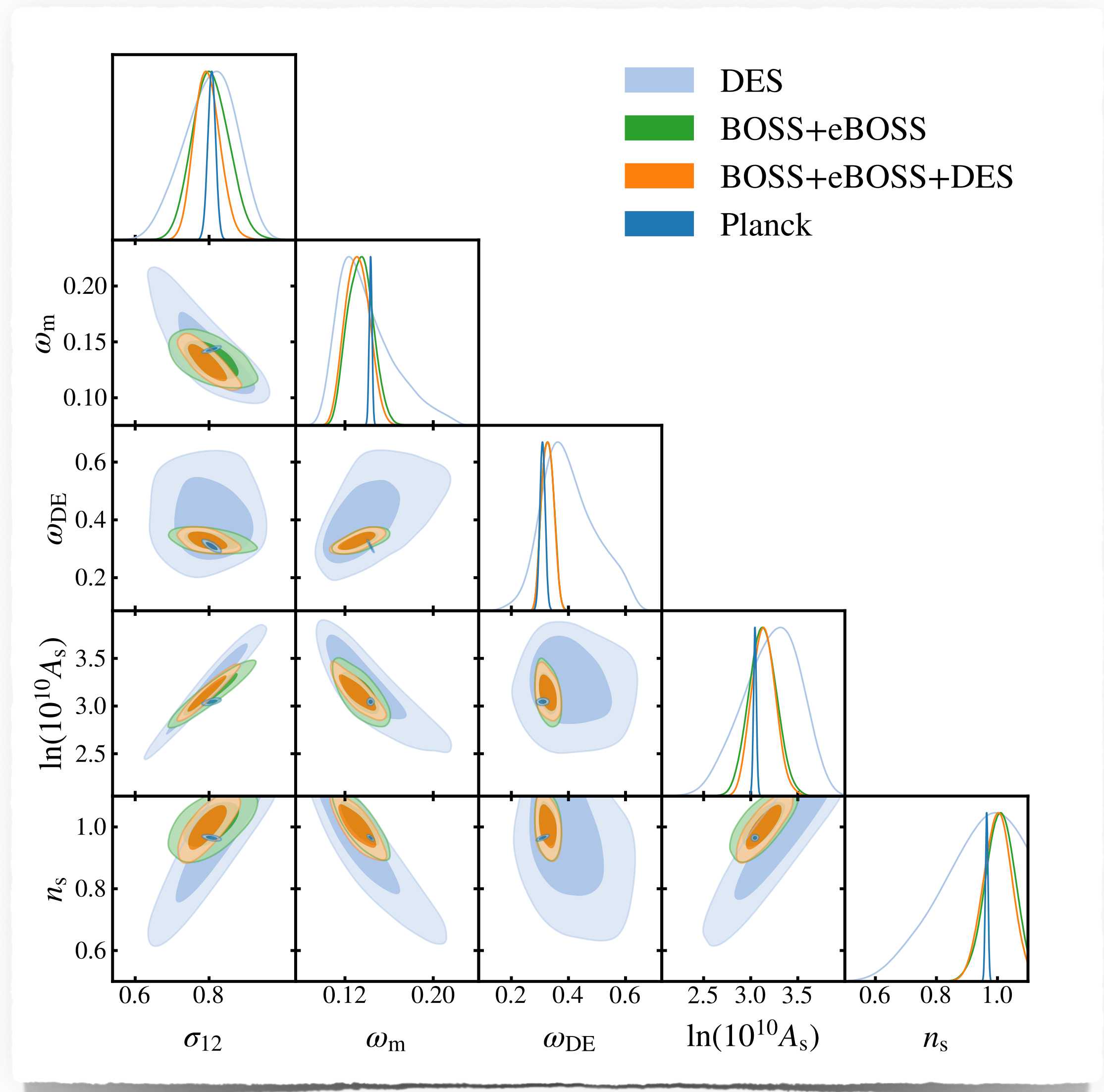
- We want to test the effect of a prior on **shape** parameters ω_b , ω_{cdm} and n_s .
- We explore the impact it has on **evolution** parameters σ_{12} , A_s , ω_{DE} .



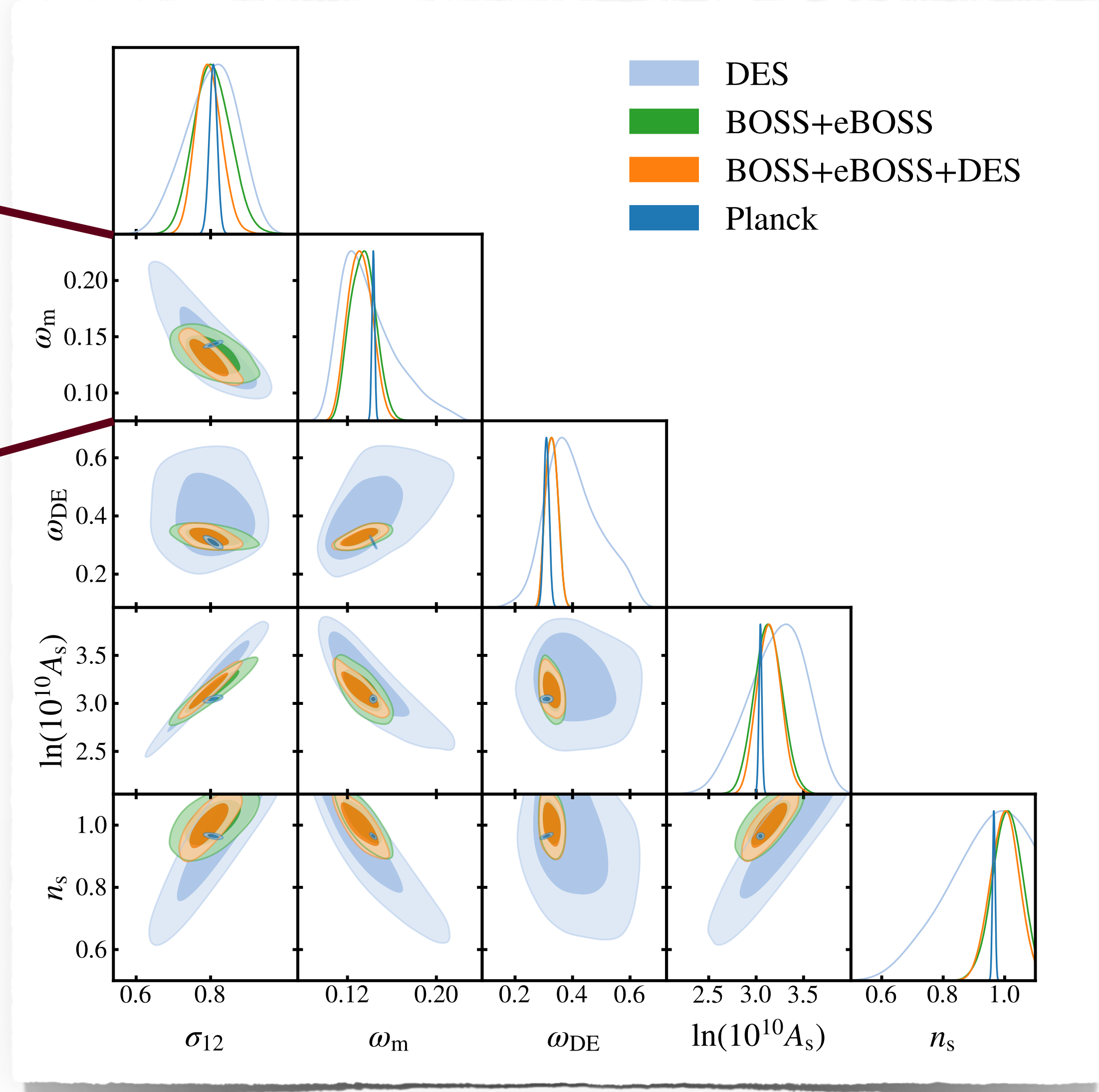
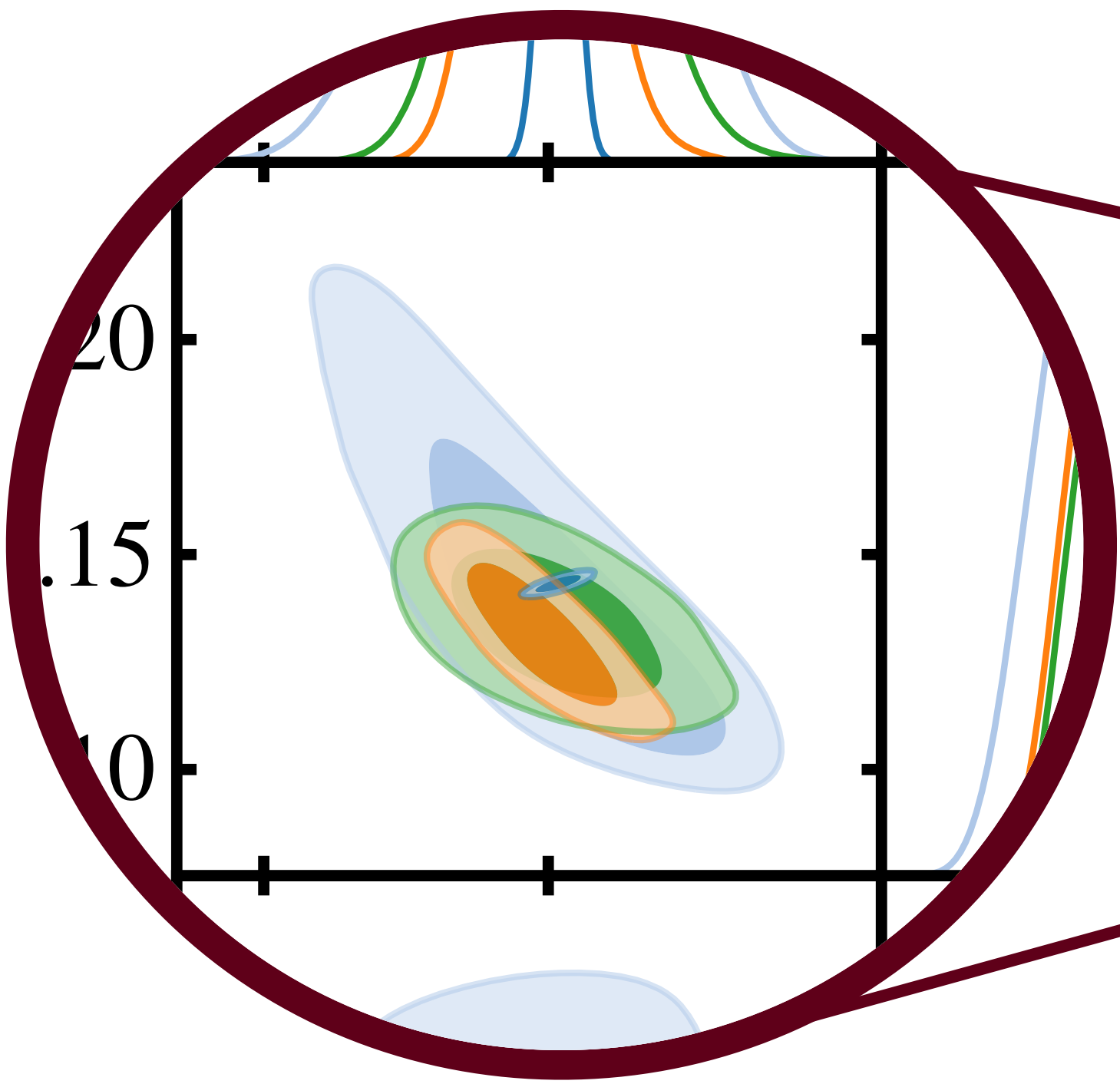
Results: BOSS+eBOSS+DES

Adding DES slightly degrades the agreement with Planck:

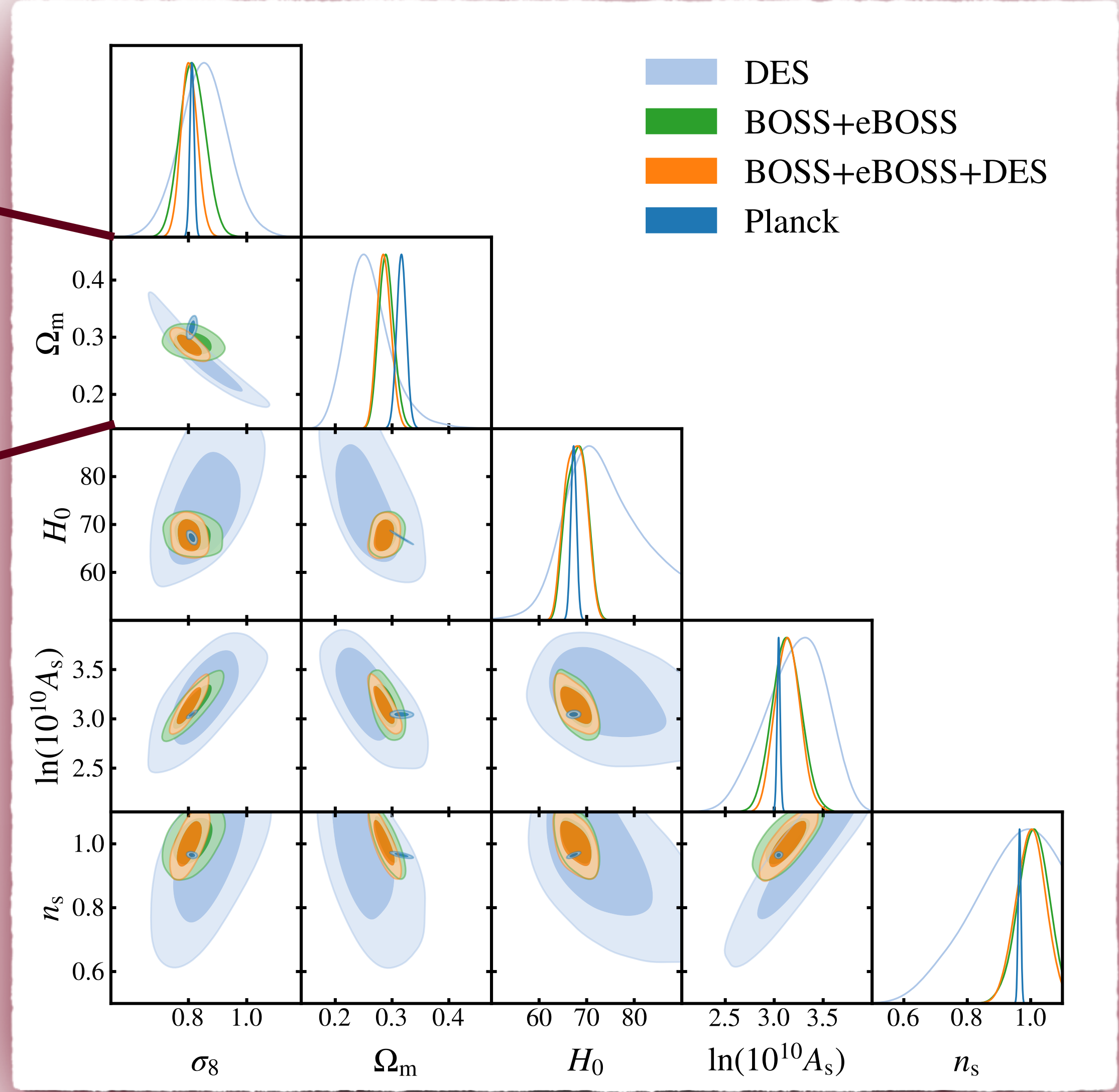
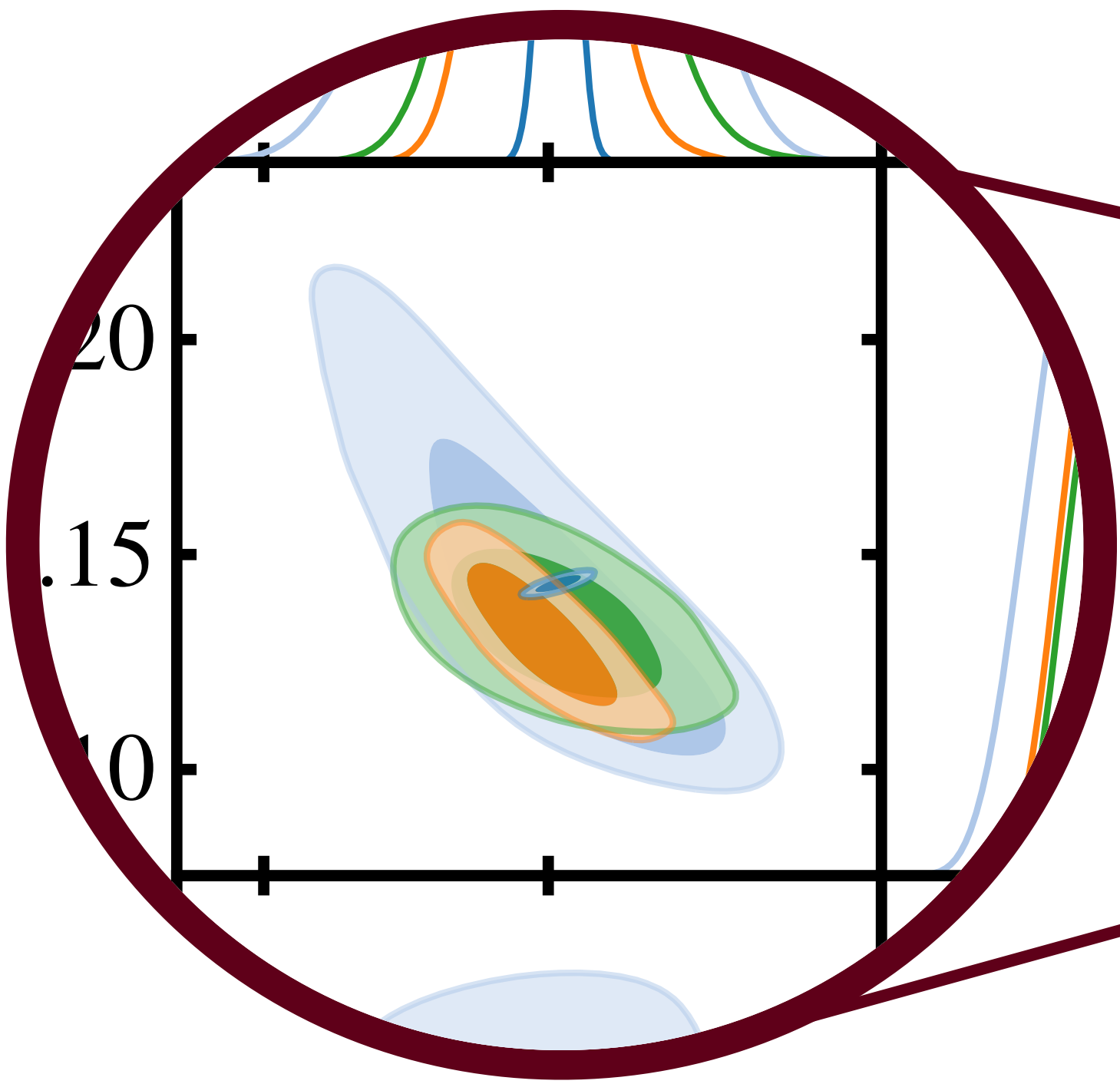
● Suspiciousness: $1.54 \pm 0.1\sigma$



Results: BOSS+eBOSS+DES



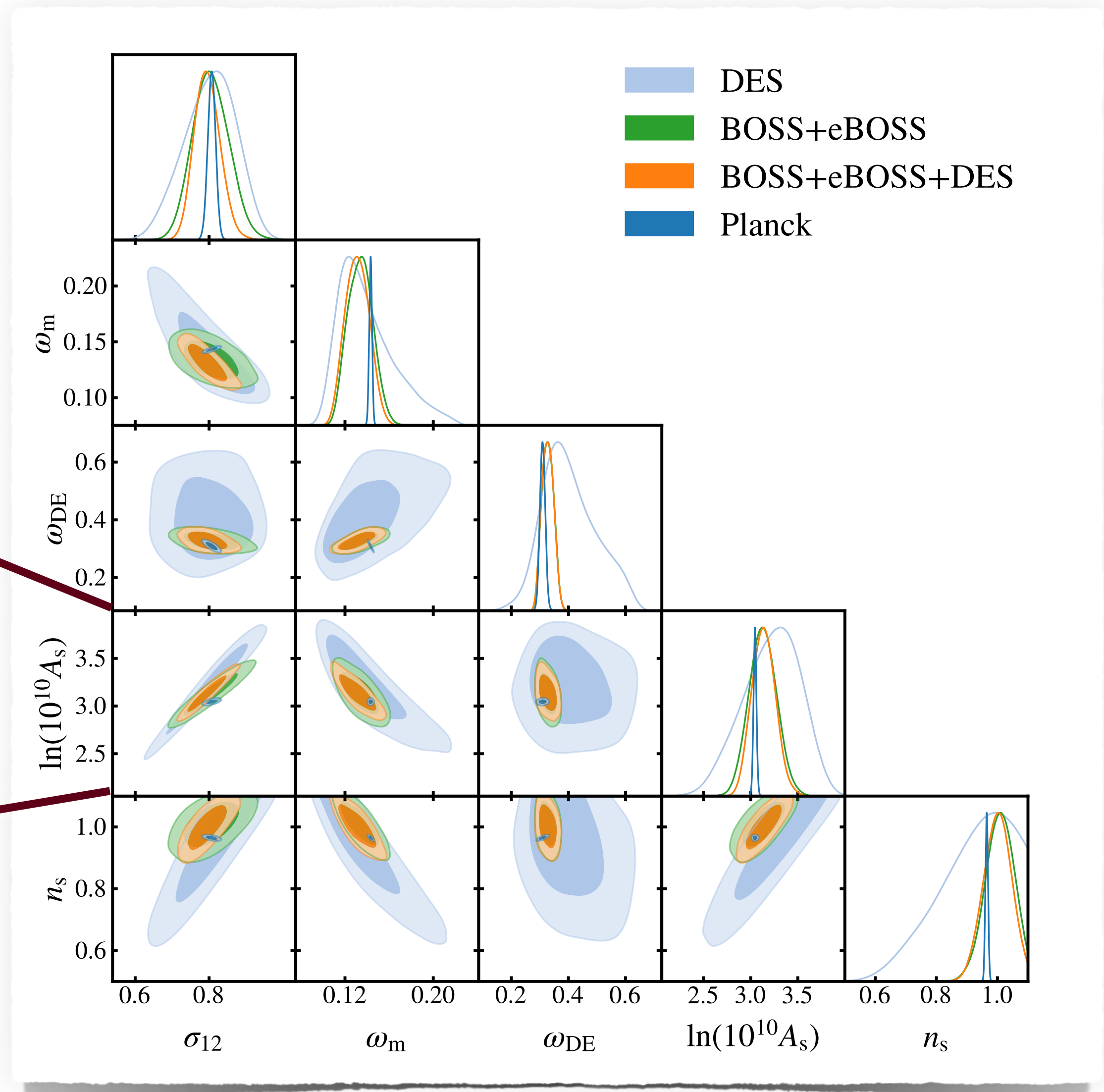
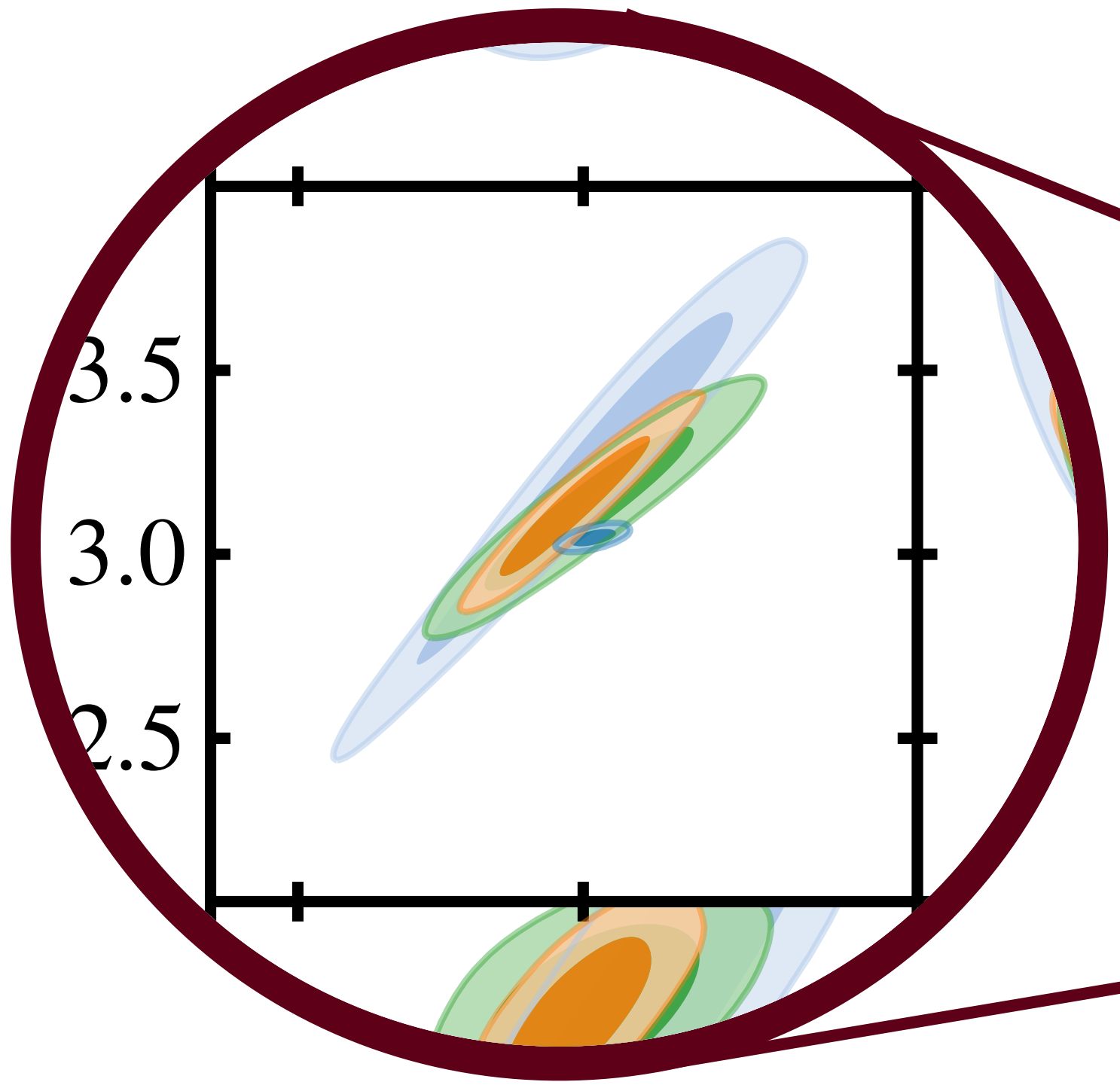
Results: BOSS+eBOSS+DES



⦿ The discrepancy in $\Omega_m - \sigma_8$ space for weak lensing appears when Mpc/h units are used.

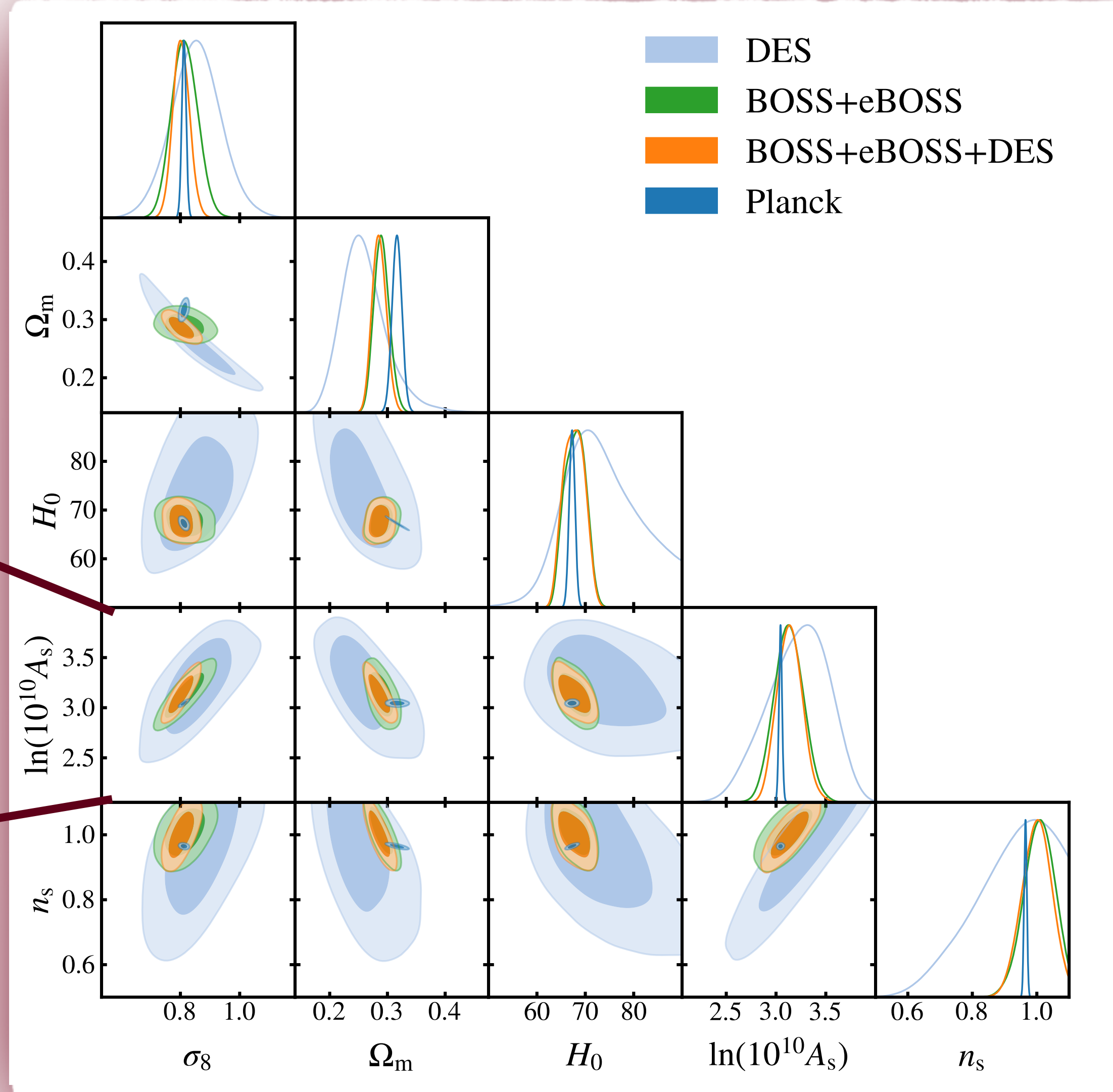
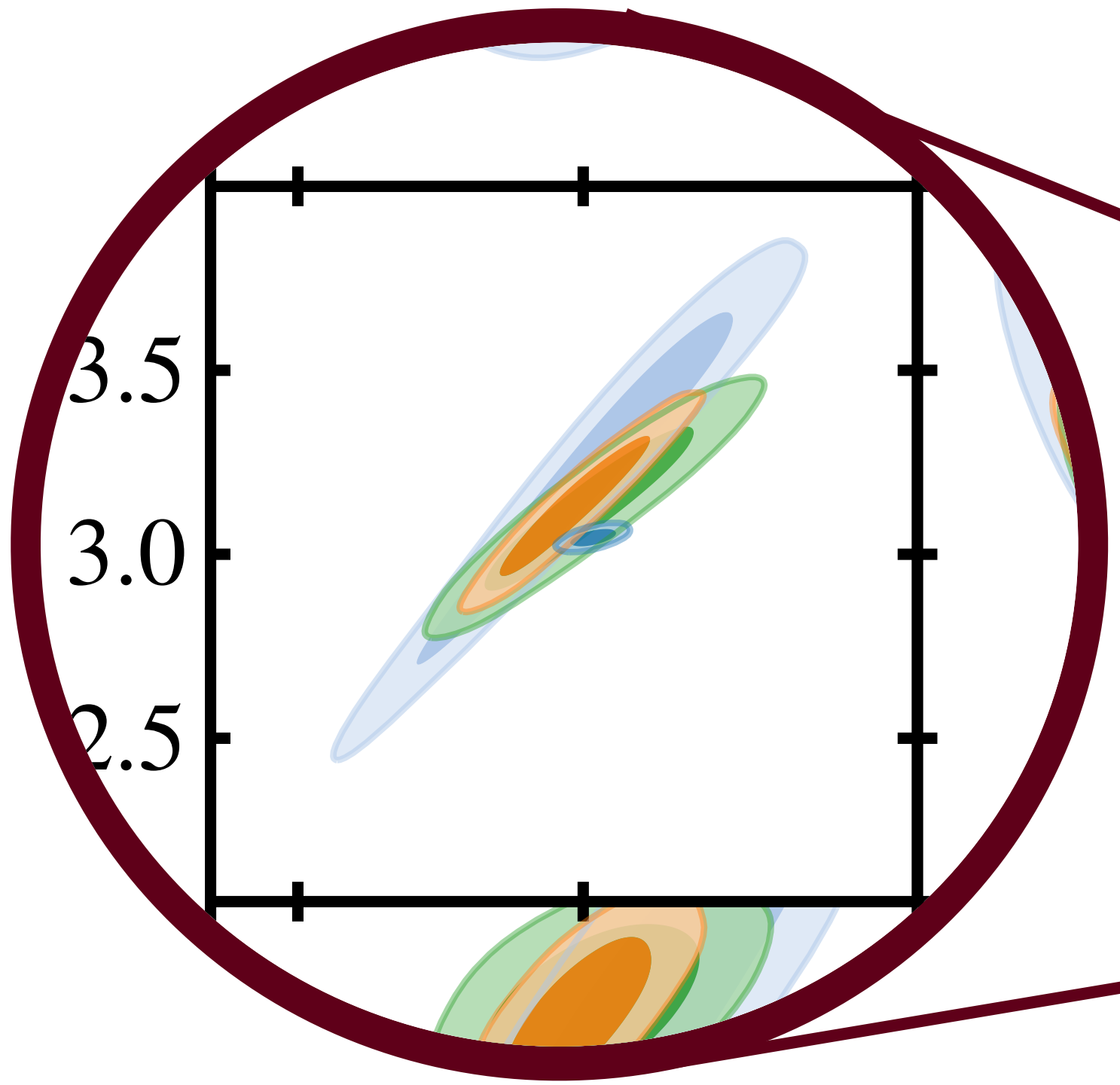
Results: BOSS+eBOSS+DES

- Planck prefers slightly *more total structure growth* than the large scale structure probes.



Results: BOSS+eBOSS+DES

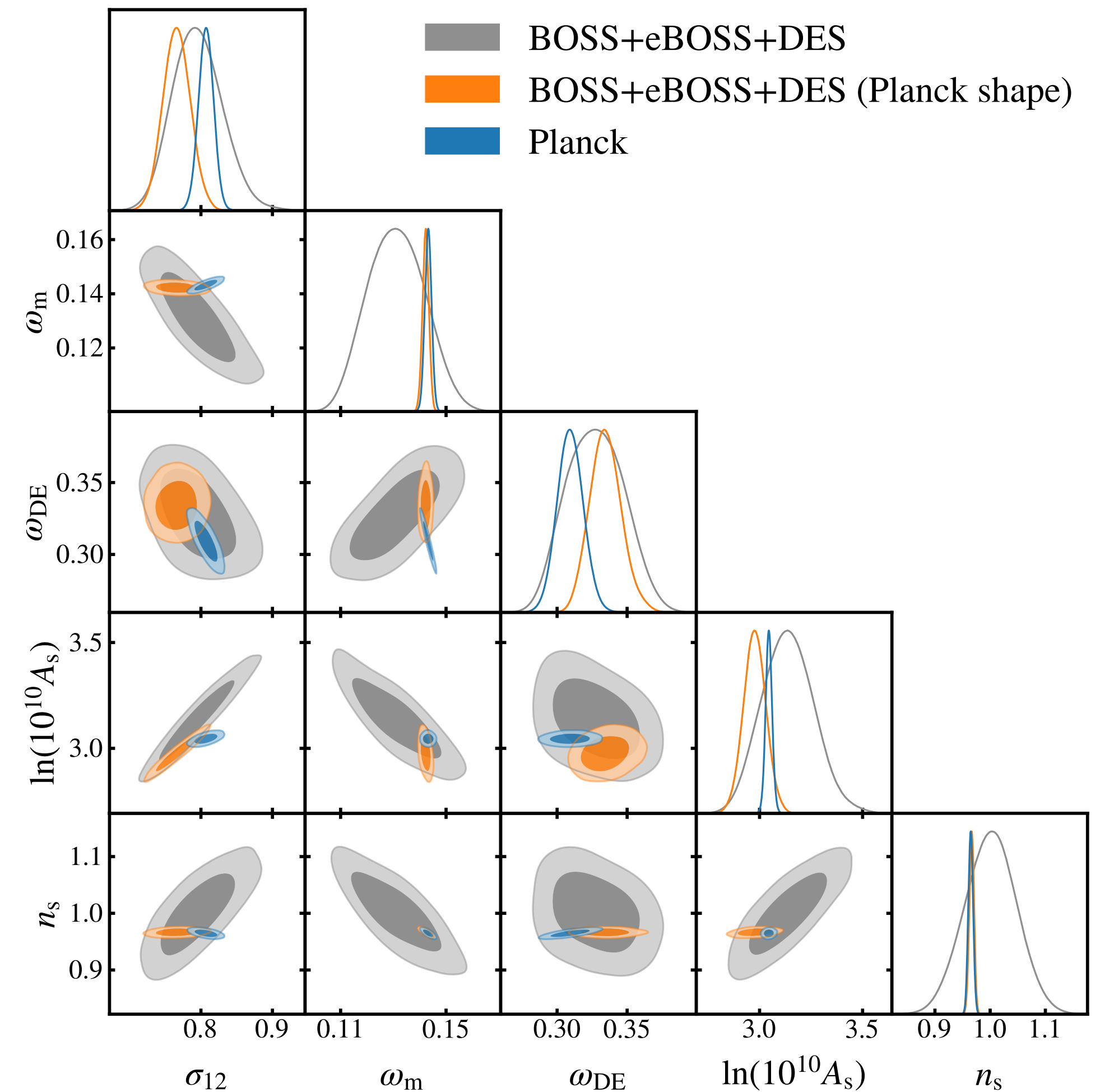
- Planck prefers slightly more total structure growth than the large scale structure probes.



Results: BOSS+eBOSS+DES

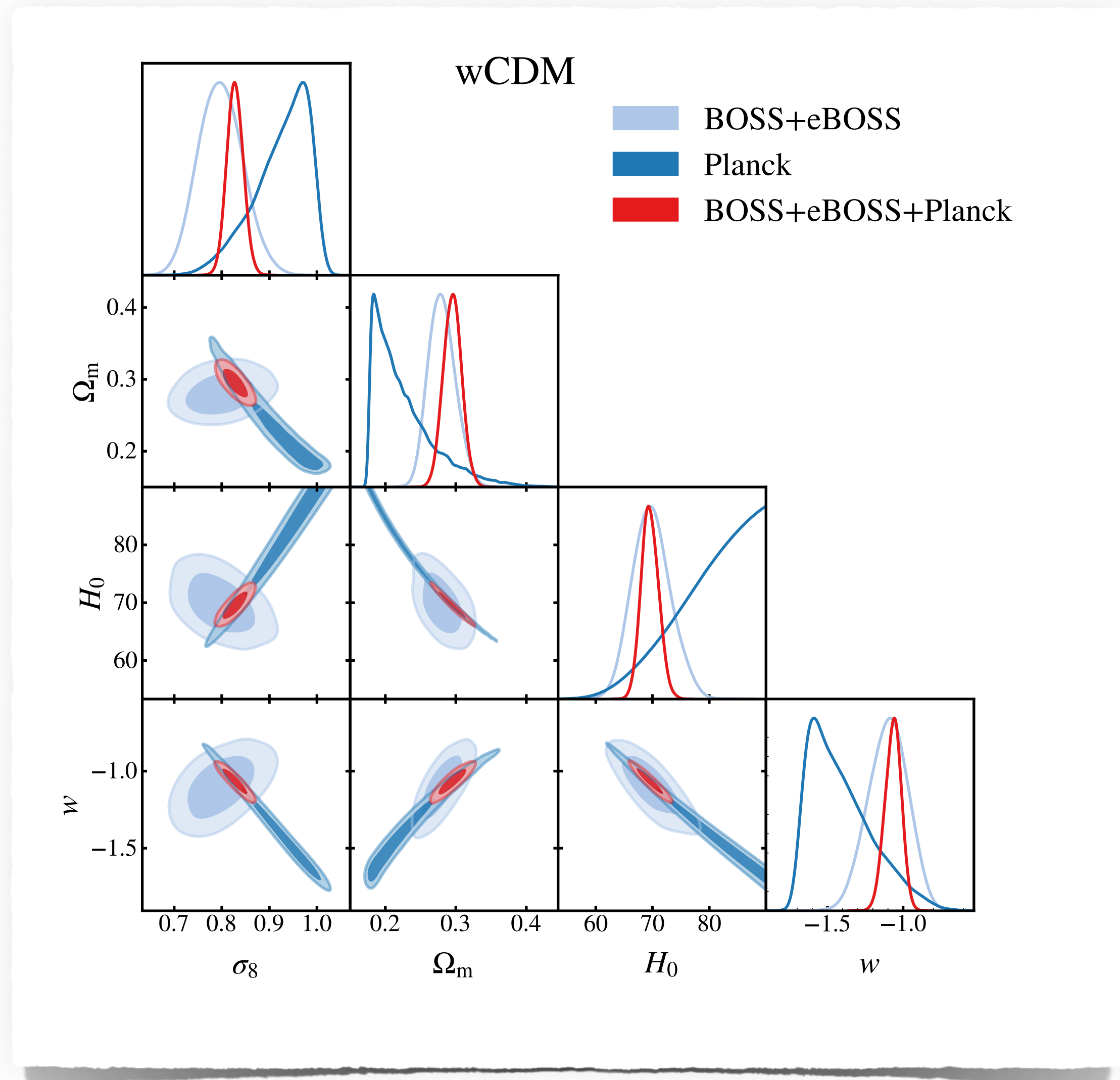
⦿ Fixing the shape parameters tightens the constraints on σ_{12} and A_s , which are subsequently given to be 1.89σ and 1.22σ below Planck values.

⦿ ω_{DE} is recovered to be 1.73σ higher than Planck.

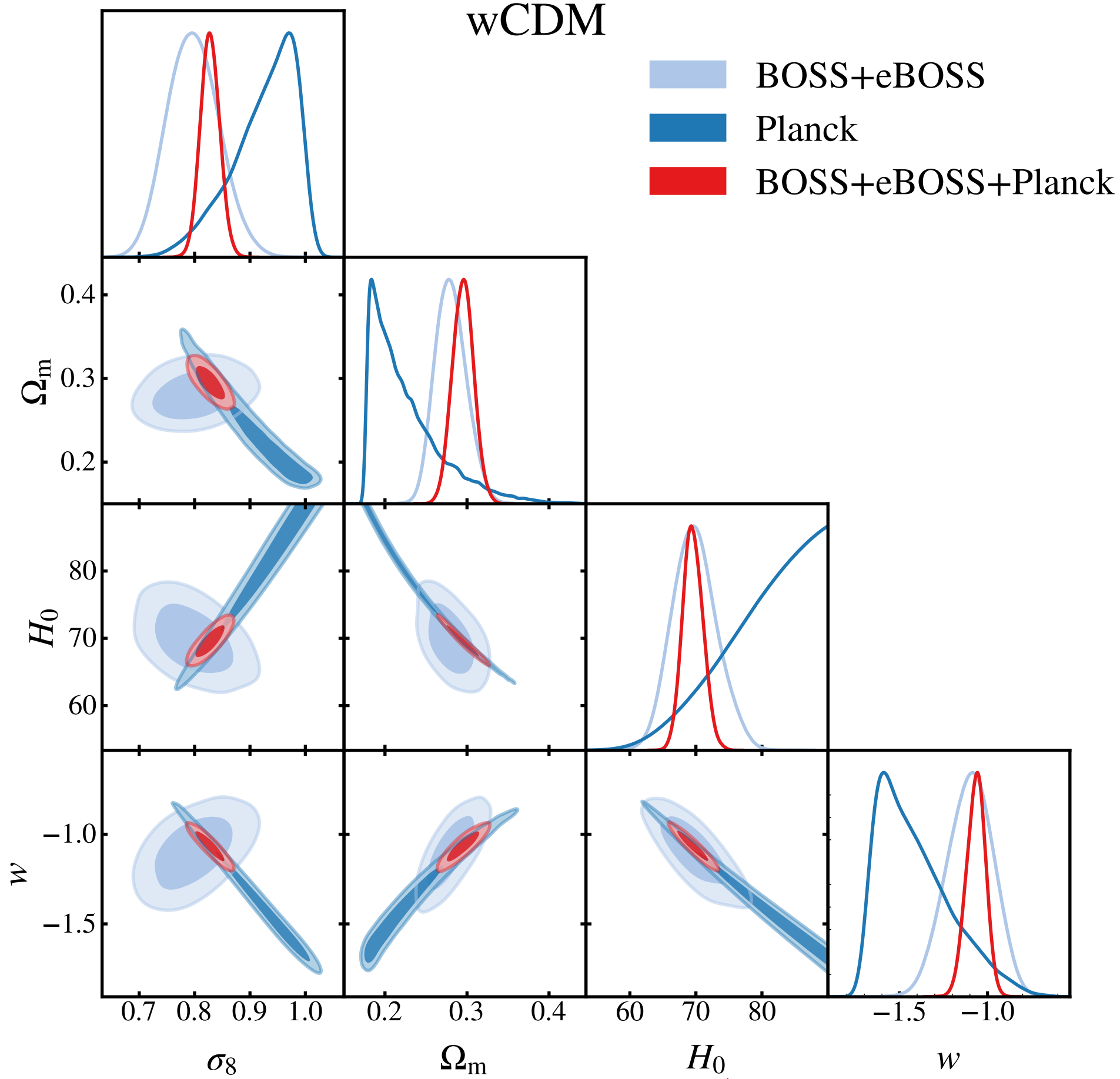
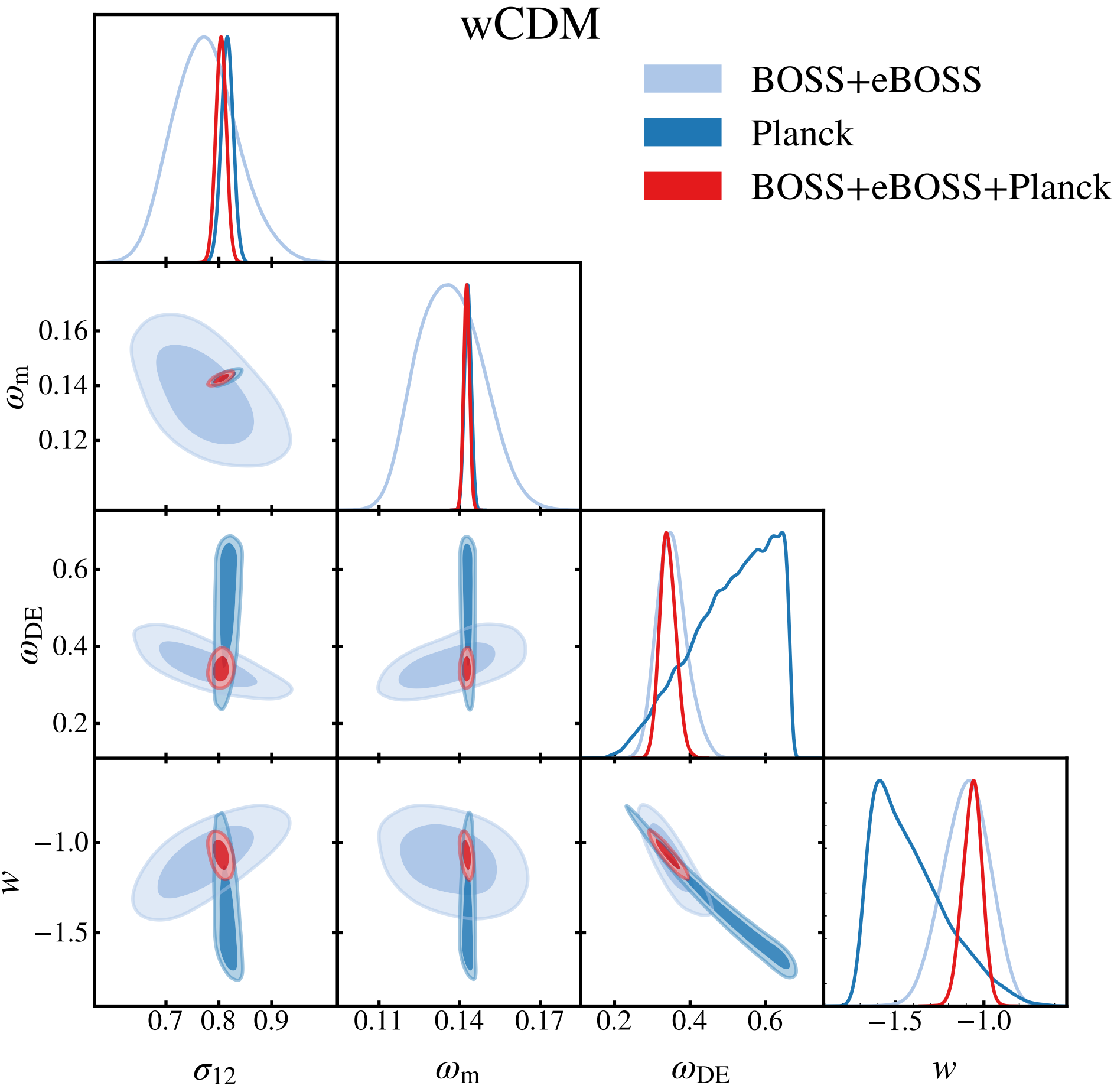


w CDM: constraining alternative dark energy models

wCDM: constraining alternative dark energy models



wCDM: constraining alternative dark energy models

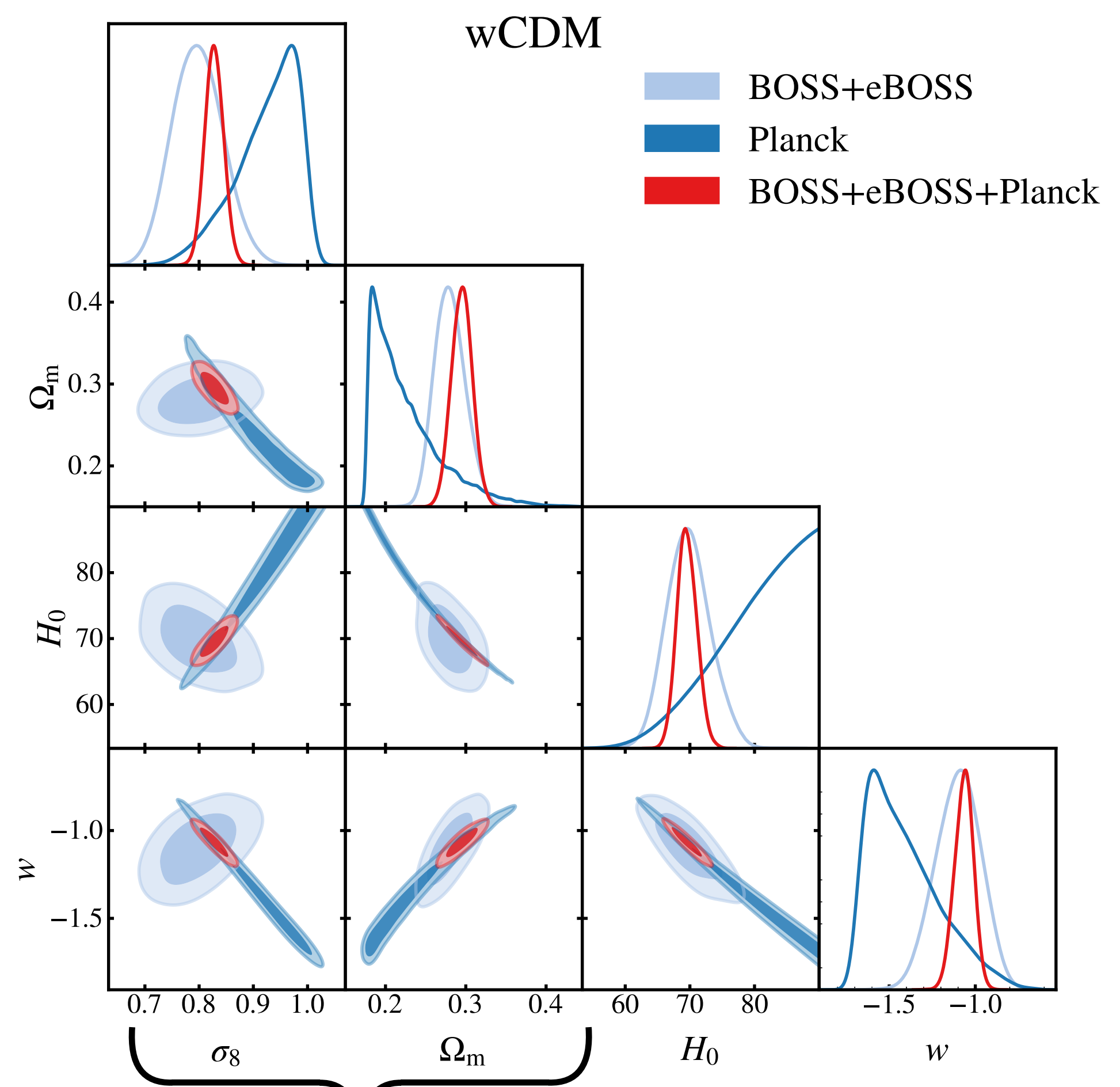
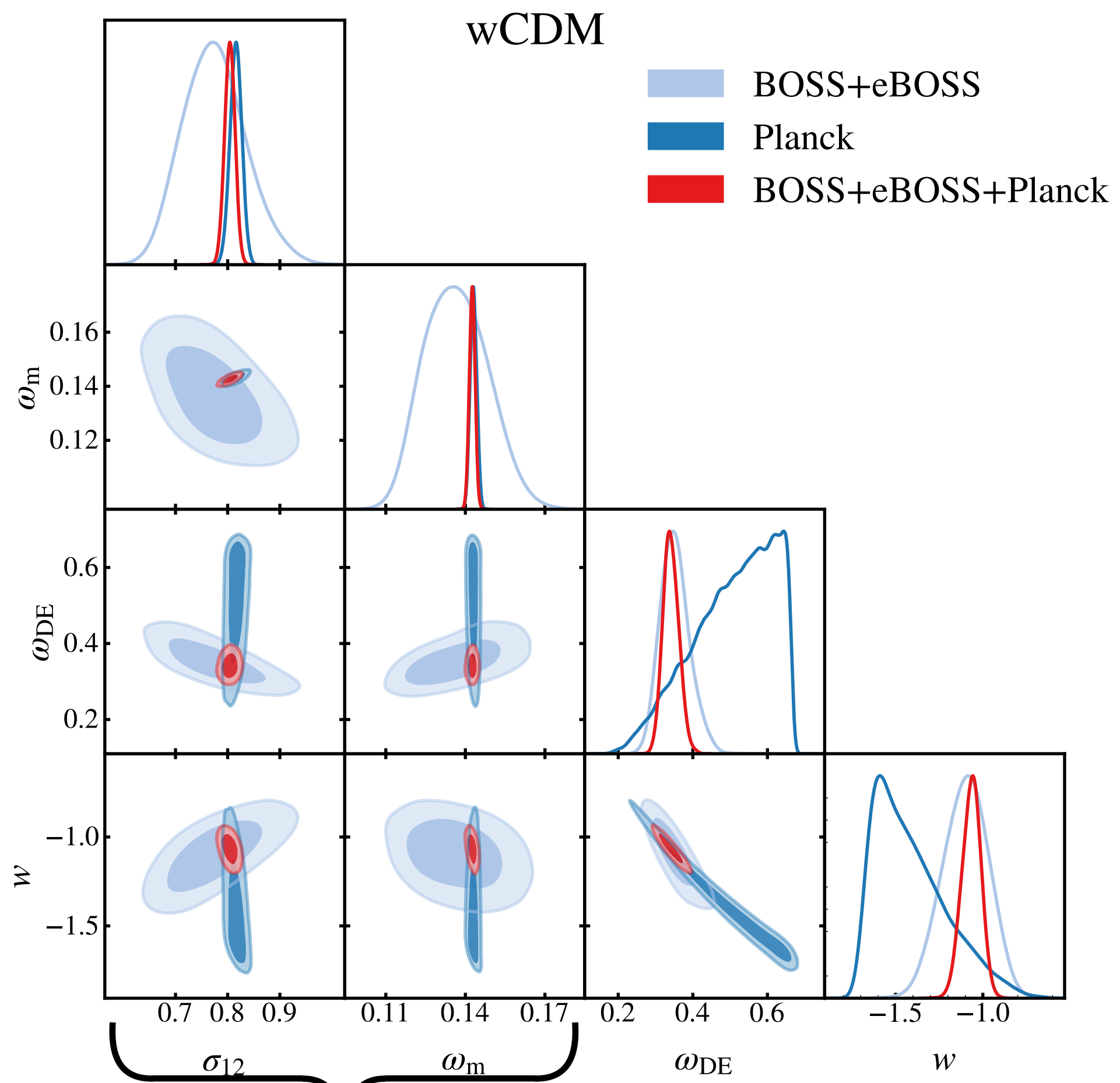


The degeneracies in H_0 are due to unconstrained ω_{DE}



(Semenaitte et al., in prep)

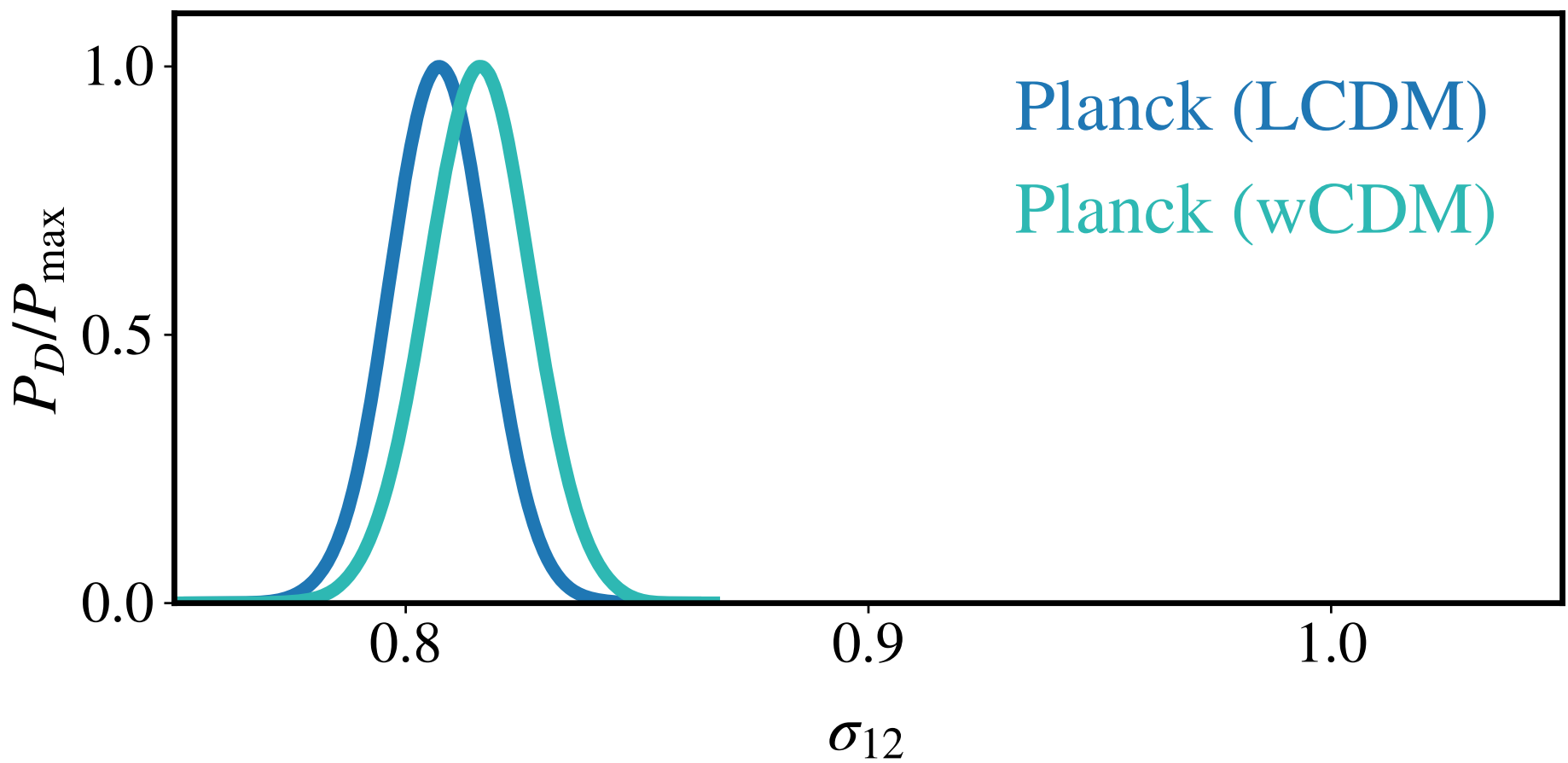
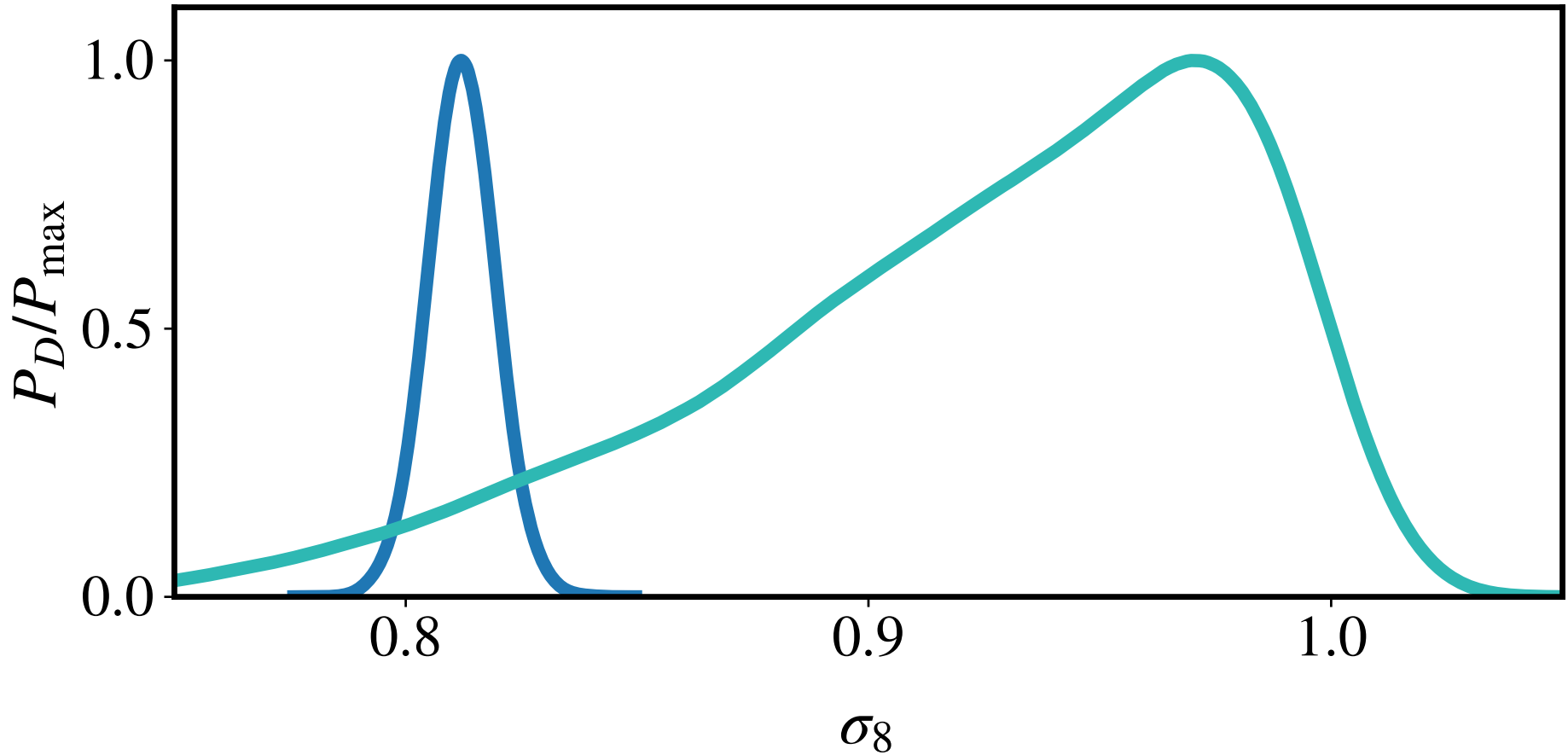
wCDM: constraining alternative dark energy models



But Planck *does constrain* ω_m and σ_{12} even with evolving dark energy!

wCDM: constraining alternative dark energy models

• First Planck constraint on power spectrum amplitude today in wCDM cosmology!



$$\sigma_{12} = 0.816 \pm 0.011 \quad \text{wCDM}$$
$$(\sigma_{12} = 0.807 \pm 0.011) \quad \Lambda\text{CDM}$$

Summary:

- We analyse the full shape of anisotropic clustering measurement from eBOSS quasar and BOSS galaxy samples.
- We find consistency between the clustering measurements and Planck within $\sim 0.6\sigma$ ($\sim 1.5\sigma$ when DES is added), as measured by the suspiciousness statistic.
- When imposing prior on the cosmological parameters that define the shape of the linear matter power spectrum we find a preference for a higher ω_{DE} by the low-redshift data sets, as compared to Planck.
- We show that CMB does constrain clustering amplitude today, even within varying dark energy models and present the first Λ CDM Planck linear density field variance constraint $\sigma_{12} = 0.816 \pm 0.011$.

